Chapter 6

Drying characteristics and optimization of process parameters in vacuum drying of culinary banana

The Chapter 6 has been discussed under three sub-heads as follows:

A) Drying characteristics and assessment of physicochemical and microstructural properties of dried culinary banana

6.1 Introduction

Drying, the process of unit operation is applied to reduce the water content of various agricultural products. The purpose of reducing water content is to prolong the shelf life of the products of bio-origin by reducing water activity to a level low enough where growth of microorganisms, enzymatic reactions and other deteriorative reactions are inhibited.[1] Tahmasebi et al.[2] stated that information on the physical and thermal properties of the agricultural products, such as heat and mass transfer, diffusion, thermal conductivity and specific heat required for designing an ideal dryer. The quality of final dried product depends on the entire drying conditions; therefore it is very important to understand the drying process and to determine the drying characteristics of the sample.[3] Thin layer drying refers to the drying process in which food materials are fully exposed to the drying air under constant drying conditions of temperature and humidity. Thus, thin-layer drying simulation is the best criterion to model the food drying process.[4]

Mathematical modeling of the convective drying process employing diffusion theory can adequately described the profile of water distribution within the particular agricultural products to a solid of perfect geometry. Establishment of functional relationship between the diffusion coefficient and the moisture content is also required.[5] Studies on drying kinetics provide parameters as experimental diffusion coefficients, which can be used to predict the drying time and thus define the basic design characteristics of drying equipment.

In the diversification of food security, culinary banana could play an essential role as it is very rich in the chemical compositions. Our concern is to utilize this crop for the benefit of society in terms of nutrients, functionality and healthy diet. But the main challenge has been to preserve it with desired moisture content, as it is responsible for most of the deteriorative microbial reactions, for safe storage life and rehydration ratio during the dehydration process. Therefore the aim of this work was to investigate the thin layer drying characteristics and

determination of effective moisture diffusivity of culinary banana. In addition, the effect of drying temperature on assessment of microstructural property and other quality attributes of dried culinary banana (both pulp and peel) in terms of colour, texture, rehydration ratio, antioxidant activity and total polyphenols were evaluated.

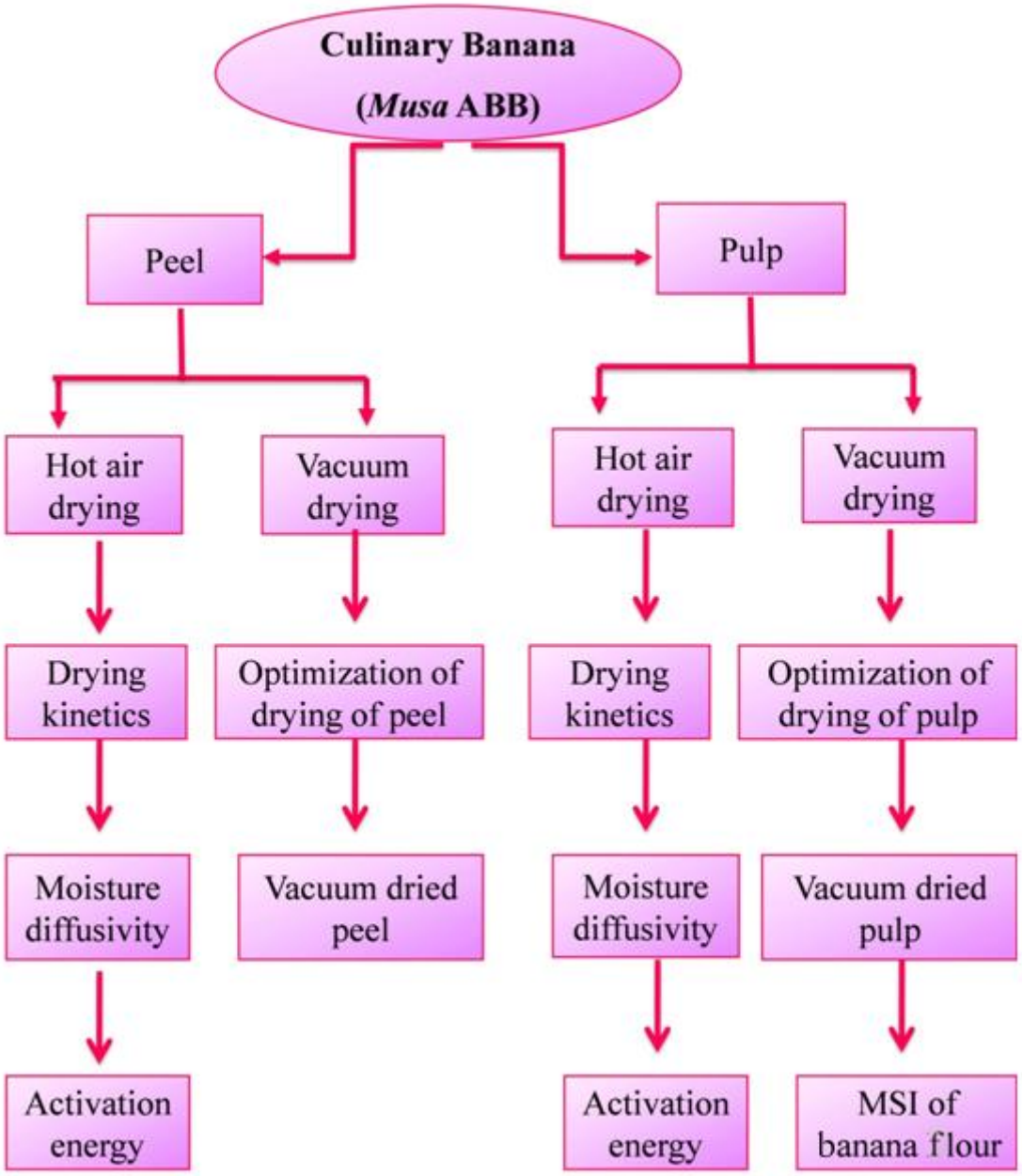

Fig 6.1 Flow chart representing drying characteristics of culinary banana peel and pulp under different drying conditions

6.2 Materials and methods

6.2.1 Sample preparation

Culinary bananas at matured edible stage were harvested from Tezpur University campus, Assam. The samples were thoroughly cleaned by washing with tap water and wiped with tissue paper before peeling to remove any dirt or dust particles attached to the peel surface. Before starting the drying experiments, the initial moisture content of both pulp and peel was measured separately by convectional hot air oven drying method at 70^{o}C for 24 h as described by Rangana.[6] The fresh and dry weights were measured with an electronic weighing balance (CPA225D, Sartorius AG, Germany) having 0.001g accuracy.

6.2.2 Experimental procedure

The thin-layer drying experiments of culinary banana pulp and peel was carried out as trial runs before optimizing the process parameters by vacuum drying. The sorted cleaned samples were peeled using stainless steel (s.s.) knife and both pulp and peel were dipped separately in solution of 1% citric acid for 15 min in order to inactivate enzymatic browning. The pulp portion was sliced into 8 mm thickness with the help of a self-designed manual slicer (Fig. 6.2). The slicer consisted of a wooden plank on top of which one movable s.s. knife was attached. The scale was fixed at both sides of cutting area and the clamp was attached and it helped the scale to move backward or forward in order to adjust the thickness of the sample. The uniform thickness of samples 8 mm (±0.01 mm) was maintained with the help of the scale attached to the slicer. On the other hand, peels were cut into small pieces and grounded into fine paste by using mechanical grinder (GX6, Bajaj, India) and paste were spread into ~4 mm thickness in stainless trays. For the drying experiment a lab scale convective tray dryer (Armfield-UOP8-A, UK) was set at desired temperatures of 40, 50, 60 and 70^{o}C (Fig. 6.3). The samples were placed on trays in single layers and drying of samples was carried out at a specified temperature. The initial weight of the trays and the samples were noted and trays were placed inside the drying chamber after the steady state condition was achieved. Samples were loaded into pre-heated drying chamber and the sample trays were taken out for weighing at every 30 min interval until constant weight was achieved. Each experiment was replicated thrice and average values were taken for analysis.

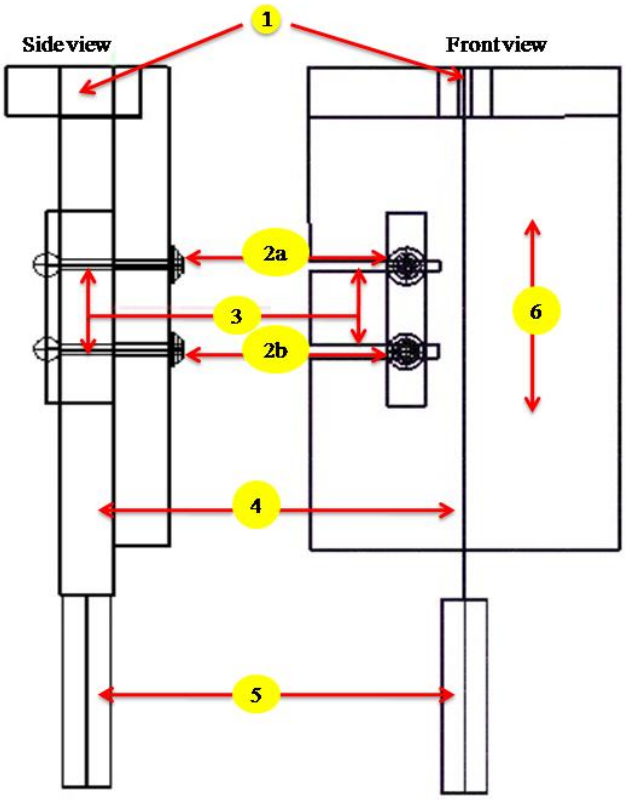

Fig. 6.2 Schematic diagram of manual slicer **(1)**: movable cutter screw, **(2a** and **2b)**: screw adjuster, **(3)**: scale bar, **(4)**: cutting blade, **(5)**: movable cutter handle

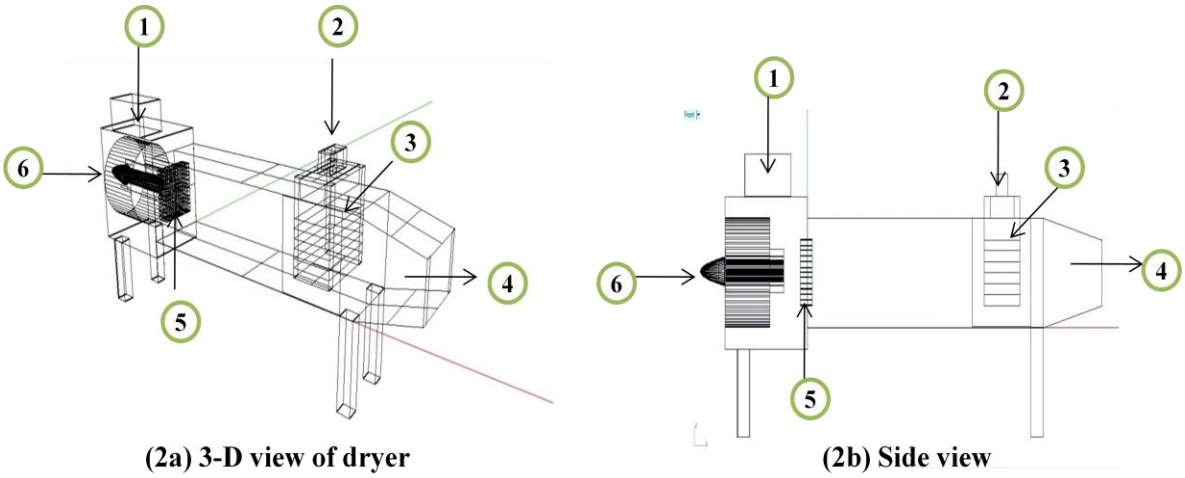

Fig. 6.3 Schematic diagrams of dryer (**1**: air and temperature controlling valve, **2**: balance, **3**: sample holding trays, **4**: air outlet, **5**: heating mantle, **6**: air circulating fan)

6.2.3 Drying kinetics

A number of theoretical, semi theoretical and empirical drying models have been reported in the literature. The Newton equation is most widely and frequently used mathematical model for describing thin-layer drying kinetics of material.[7, 8] As drying proceeds, the moisture content of the material decreases and the mechanism of drying changes, which is controlled by liquid diffusion mechanism described by Fick's second law. The solution of the Fick's equation, with the assumptions of diffusion based moisture migration, negligible shrinkage, constant diffusion coefficients and temperature is simplified to get the single exponential model as described by Lewis[9] as:

$$MR = \frac{M_t - M_e}{M_i - M_e} \quad \text{Eq. (6.1)}$$

Where, MR = Moisture Ratio; M_i = initial moisture content ($kg_{water}/kg_{dry\ matter}$); M_t = moisture content at time t ($kg_{water}/kg_{dry\ matter}$); M_e = equilibrium moisture content ($kg_{water}/kg_{dry\ matter}$).

The drying data of MR versus drying time was analyzed for nine thin-layer drying models given in Table 6.1 to select the best model to describe the thin layer drying curve. All the statistical analysis was done using statistical software OriginPro 8.5 (OriginLab Corporation, Northampton, USA). The reduced chi-square value (χ^2) and adjusted coefficient of determination value (R^2) were used as the primary criteria to select the best equation to account for variation in the drying curve of samples. The reduced chi-square value (χ^2) is the mean square of the deviations between the experimental and calculated values for the models and used to determine the goodness of fit. For quality fit, R^2 values should be higher and χ^2 values should be lower.[10]

Table 6.1 Mathematical models used for thin-layer drying of culinary banana

Model	**Mathematical Equation**	**References**
Lewis	MR = exp (-kt)	Doymaz[11]
Page	MR = exp ($-kt^n$)	Page[12]
Modified Page	MR = exp $(-kt)^n$	Yaldiz et al.[13]
Henderson and Pabis	MR = a exp (-kt)	Henderson and Pabis[14]
Logarithmic	MR = a exp (-kt) + c	Togrul and Pehlivan [15]

Two-Term Model	MR = a exp ($-k_0t$) + b exp ($-k_1t$)	Rahman et al.[16]
Approximation of Diffusion	MR = a exp (-kt) + (1-a) exp (-kmt)	Lahsasni et al.[17]
Wang and Singh	MR = 1 + at + bt^2	Wang and Singh[18]
Modified Page Equation II	MR = exp [$-c\ (t/L_c^2)^n$]	Doymaz[11]

6.2.4 Effective moisture diffusivity

The drying material is considered as a thin slab of thickness L = 2b at uniform initial temperature (T_0) and initial moisture content (M_i) because the two sides are exposed to an airflow at temperature (T_a) and relative humidity (RH). Assuming uniform initial moisture content and negligible external resistance the Fick's diffusion equation for object with slab geometry was used for calculation of effective moisture diffusivity. The following assumptions were considered for the effective moisture diffusivity for an infinite slab.[19]

(a) Moisture is initially distributed uniformly throughout the mass of a sample.

(b) Mass transfer is symmetric with respect to the centre.

(c) Surface moisture content of the sample instantaneously reaches equilibrium with the condition of surrounding air.

(d) Resistance to the mass transfer at the surface is negligible compared to internal resistance of the sample.

(e) Mass transfer is by diffusion only.

(f) Diffusion coefficient is constant and shrinkage is negligible.

$$MR = \frac{M_t - M_e}{M_i - M_e}$$

$$= \frac{8}{\pi^2} \sum_{n=0}^{\infty} \frac{1}{(2n+1)^2} \exp\left(-\frac{(2n+1)^2 \pi^2 D_{eff}\, t}{4L^2}\right) \qquad \text{Eq. (6.2)}$$

Where MR is moisture ratio, M_t is the moisture content at any time ($kg_{water}/kg_{dry\ matter}$), M_i is the initial moisture content ($kg_{water}/kg_{dry\ matter}$), n = 0, 1, 2, 3.....the number of terms taken into consideration, D_{eff} is the effective moisture diffusivity (m^2/s), L is the sample thickness (mm) and t is the drying time (min). The moisture diffusivity was estimated by plotting the natural logarithm of moisture ratio (ln MR) with respect to drying time (t) at various temperatures.

6.2.5 Activation energy

The activation energy was calculated using an Arrhenius type equation given below[20, 21]

$$D_{eff} = D_0 \exp\left(-\frac{E_a}{R(T+273.15)}\right) \quad \text{Eq. (6.3)}$$

Where D_0 is the pre-exponential factor of the Arrhenius equation, E_a is the activation energy (kJ/mol), R is the ideal gas constant (8.314 J/Kmol) and T is the drying temperature. The above Eq. (3) can be written as

$$\ln(D_{eff}) = \ln(D_0) + \left(-\frac{E_a}{R(T+273.15)}\right) \quad \text{Eq. (6.4)}$$

The activation energy can be obtained from the slope of the Arrhenius plot, ln (D_{eff}) versus $1/T_{abs}$, from Eq. (4) a plot of ln (D_{eff}) versus $1/T_{abs}$ gives a straight slope of K

$$K = -\frac{E_a}{R} \quad \text{Eq. (6.5)}$$

6.2.6 Physicochemical analysis

6.2.6.1 Microstructure evaluation

The microstructure of culinary banana slices and peel dried at different temperatures was studied in scanning electron microscope (JEOL JSM-6390LV, SEM, Oxford) following the method described by Thuwapanichayanan et al.[22] Sample micrographs were observed at a magnification of 250X at an accelerating voltage of 15 kV.

6.2.6.2 Texture analysis

The textural property of dried culinary banana slices was determined in terms of hardness following the method explained by Alvaraz et al.[23] The measurement of hardness was evaluated using a Texture Analyzer (TA-HD Plus, Stable Micro Systems, UK). The dried banana samples were tested using 1/4" diameter ball probe using 2500 N load cell. The pipe cylinder with an outside diameter of 25 mm and inside diameter of 18 mm was mounted on the plate component of the texture analyzer to support the banana slice for test. The measurement settings on the texture analyzer were set at pre-test speed of 1 mm/s and test speed of 5 mm/s. The hardness is the amount of maximum force required to break the sample to form a deformation curve and

represented as the first force peak if there are only two peaks found, or the second peak if there are three peaks found on the TPA curve.

6.2.6.3 Nonenzymatic browning

The nonenzymatic browning of dried samples was determined in terms of optical index (OI) following the method given by Samaniego-Esguerra.[24] Briefly, dried sample (15g) was extracted in 50 ml of 95% ethanol and 50 ml of distilled water. The mixture was kept inside the shaker (New Brunswick Scientific, Excella E24 Incubator Shaker) at 25^{o}C and 250 rpm for 60 min for uniform mixing followed by centrifugation at 2500 rpm for 20 min using refrigerated centrifuge (SIGMA Laborzentrifugen, 3-18 KS, Germany). Supernatant (10 ml) was taken and 95% ethanol (10 ml) was added to it and mixed thoroughly. The mixture was then filtered using Whatman No. 4 filter paper, the filtrate was again refiltered through Whatman No. 42. The absorbance of clear filtrate was measured at 420 nm wavelength and 5 cm cell path length using UV visible spectrophotometer (Spectrascan UV-2600, Thermo Fisher Scientific, India). The Optical Index (OI) was measured using following equation

$$OI = \frac{\text{absorbance} \times 5 \times 1000}{b' \times w} \qquad \text{Eq. (6.6)}$$

Where, b' = cell path used, w = weight of sample (g)

6.2.6.4 Rehydration ratio

The rehydration ratios of dehydrated samples were measured following the method for rehydration test of fruits and vegetables of Ranganna[6]. The weights of the sample before and after the rehydration were measured and the rehydration ratio was determined using the following formula:

$$\text{Rehydration ratio} = \frac{\text{weight of the sample (g) after rehydration}}{\text{weight of the sample (g)before rehydration}} \qquad \text{Eq. (6.7)}$$

6.2.6.5 Determination of DPPH radical scavenging activity and total polyphenols

The free radical scavenging activity of dried samples was determined following the method given by Brand-Williams et al.[25] and total polyphenols were measured following the method of Malick and Singh[26] (method described in section 2.2.2.5).

6.2.7 Statistical analysis

Experiments were carried out in three replicates. The data analysis tool 'Microsoft Excel' was used for all the statistical analyses and standard deviations are presented in the results. Data were subjected to ANOVA and Fisher's Least Significant Difference (LSD) was used to separate means.

6.3 Results and Discussion

6.3.1 Drying characteristics

The thin-layer drying of culinary banana pulp slices and peel paste exhibited falling rate period. The slice thickness of the pulp was 8 mm and the initial moisture content was in 588.32 kg water/kg dry solids (or 85.47% wb) which was reduced to 11.85 kg water/kg dry solids (10.59% wb). On the other hand, thickness of peel paste was ~ 4 mm and its initial moisture content was recorded 582.30 kg water/kg dry solids (or 85.30% wb) and after drying it reduced to 10.87 kg water/kg dry solids (9.80% wb). The moisture content decreased at various temperatures of 40, 50, 60 and 70^{o}C with elapsing of time. The drying rate of samples was calculated from the drying data by estimating the change in moisture content at specific time interval. The value of moisture ratio was obtained using Eq. (6.1). The relation between moisture ratio and drying time for all the four drying temperatures rare illustrated in Fig. 6.4a and Fig. 6.4b for pulp and peel respectively. As the drying process progressed, the moisture ratio decreased non-linearly with increase in drying time. It was observed (Fig. 6.4a) that sample at 40^{o}C took nearly 20 h (1200 min) of drying time to reduce moisture content of the sample from 588.32 to 11.85 kg water/kg dry solids and evinced that with increase in drying temperature the

drying time also got decreased. Similarly, peel paste required a total time of nearly 16.6 h (1000 min) to reduce moisture content from 582.30 to 10.87 kg water/kg dry solids. As the temperature was increased to 70^{o}C the same thickness of banana slices (8 mm) and peel paste (4 mm) required less than 5 h (for pulp) and 3 h (for peel) to reduce the same moisture content. The results are in agreement with various authors reported in fruits and vegetables viz., eggplant,[27] potato slices,[20] cassava chips,[7] peach slices[8] and ripe banana.[28]

During falling rate period, the drying process of samples was mainly controlled by diffusion mechanism.[29] The moisture ratio at each drying temperature rapidly dropped in the initial stage and then it gradually reached equilibrium moisture content. As surface moisture of the sample reduced, removal of moisture from inside the material became slower thereby requiring more energy to detach water molecules from the solid matrix. Hence the drying time required to attain equilibrium moisture content decreased as temperature increased. Similar observations have been reported for drying characteristics of ripe banana slices.[30] The drying rate curve obtained is a typical behaviour of agricultural materials that possess porous or cellular structure viz., dessert banana slices[22, 31] and potato and carrot slices.[32]

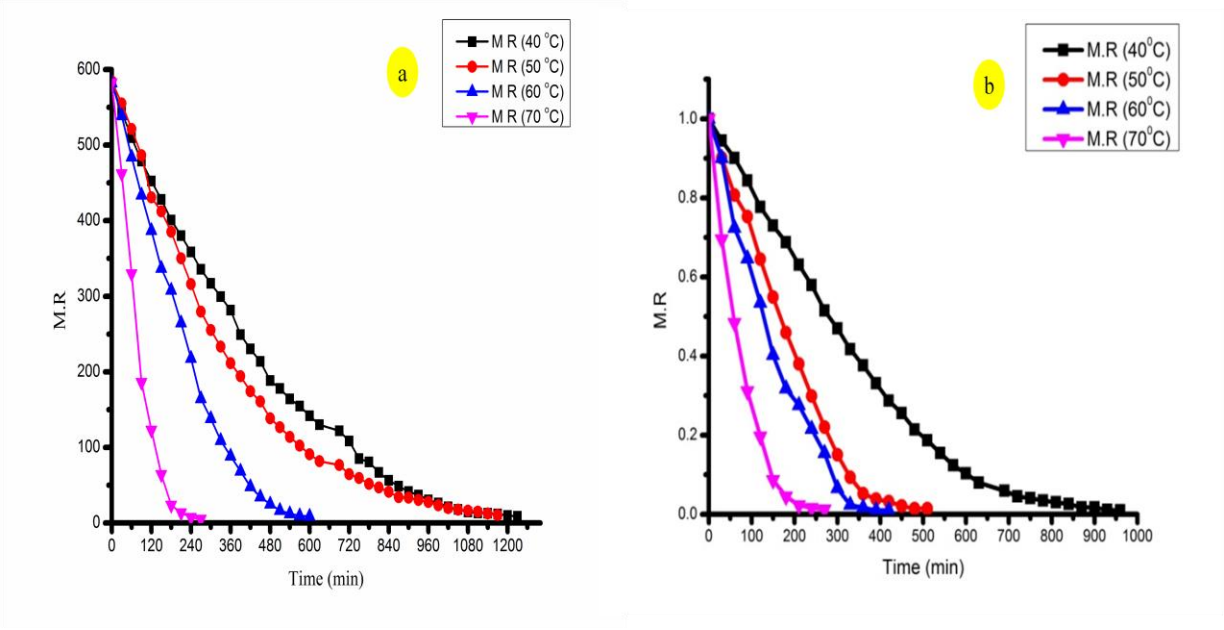

Fig 6.4 Moisture ratio vs drying time of **(a)** culinary banana pulp slices and **(b)** peel paste

6.3.2 Mathematical modeling for fitting drying curves

The moisture content data of both pulp and peel obtained at various air drying temperature was converted to moisture ratio and was fitted to different thin-layer drying models given in Table 6.1. The models were evaluated on the basis of coefficient of determination (R^2) and the reduced chi-square (χ^2). The drying model constants and coefficients from the results of statistical analysis of all models are given in Table 6.2 for pulp slices and in Table 6.3 for peel paste. For pulp slices, χ^2 and R^2 values (40-70^{o}C) varied from 2.58 x 10^{-4} to 3.89 x 10^{-3} and 0.83 to 0.99 respectively. Results evinced that (Table 6.2) in Wang and Singh model, least χ^2 (2.58 x 10^{-4}) and highest R^2 (0.99) values were obtained and gave a better correlation between moisture ratio and drying time over the other models fitted (Fig. 6.5a) and therefore is more precise to describe thin-layer drying of culinary banana pulp slices. From Table 6.3 it can be seen that in case of culinary banana peel, the average value of χ^2 varied from 2.23 x 10^{-4} to 8.44 x 10^{-2} and value of R^2 varied between 0.80-0.99. Therefore, from Table 6.3 it can be concluded that modified Page model was found to be the best fitted model with least χ^2 value of 2.23 x 10^{-4} and highest R^2 value of 0.99, thus modified Page model was selected as suitable model to represent the thin-layer drying behaviour of peel paste and it is illustrated in Fig. 6.5b.

Table 6.2 Values of model constants for thin-layer drying of culinary banana slices

Drying temperature 40°C			
Model name	**Coefficients and constants**	**χ^2**	**R^2**
Lewis/Newton	k = 0.0023	1.370×10^{-3}	0.9846
Page			0.9160
Modified Page	k = 0.0023, n = 1.2097	1.975×10^{-4}	0.9952
Henderson and Pabis	a = 1.0498, k = 0.0024	1.112×10^{-3}	0.9871
Logarithmic	a = 1.1380, c = -0.1328, k = 0.0018	4.691×10^{-4}	0.9981
Two-Term	a = 0.5249, b = 0.5249,k_0 = 0.0024, k_1 = 0.0024	1.212×10^{-3}	0.9864
Approximation of Diffusion	a = 2.724×10^{-6}, k = -868.277, m = 2.3681	1.446×10^{-3}	0.9837
Wang and Singh	**a = -0.0017, b = 7.731×10^{-7}**	**2.855×10^{-4}**	**0.9976**
Modified Page Equation II	c = 0.0059, L = -2.485, n = 1.205	3.961×10^{-4}	0.9955
Drying temperature 50°C			
Model name	**Coefficients and constants**	**χ^2**	**R^2**
Lewis/Newton	k = 0.0028	7.240×10^{-4}	0.991
Page			0.916
Modified Page	k = 0.0027, n = 1.1746	7.695×10^{-4}	0.991
Henderson and Pabis	a = 1.0631, k = 0.0030	3.769×10^{-4}	0.995
Logarithmic	a = 1.0823, c = -0.0365, k = 0.0027	3.215×10^{-4}	0.997
Two-Term	a = 0.5315, b = 0.7324, k_0 = 0.0030, k_1 = 0.5812	3.985×10^{-4}	0.995
Approximation of Diffusion	a = 1.296×10^{-5}, 2.237, k = -219.273	7.644×10^{-4}	0.991
Wang and Singh	**a = -0.00207, b = 1.092×10^{-6}**	**2.589×10^{-4}**	**0.999**
Modified Page Equation II	c = 0.005, L = -2.0072, n = 1.1757	5.849×10^{-4}	0.997
Drying temperature 60°C			
Model name	**Coefficients and constants**	**χ^2**	**R^2**
Lewis/Newton	k = 0.0045	3.89×10^{-3}	0.963
Page			0.920
Modified Page	k = 0.0043, n = 1.4296	3.61×10^{-4}	0.991
Henderson and Pabis	a = 1.0941, 0.0049	2.98×10^{-3}	0.972
Logarithmic	a = 1.2559, c = -0.2124, k = 0.0032	8.53×10^{-4}	0.942
Two-Term	a = 0.5486, b = 0.9470, k_0 = 0.0049, k_1 = 0.0065	3.33×10^{-3}	0.969
Approximation of Diffusion	a = -0.1714, k = 0.0305, m = 0.0445	2.27×10^{-3}	0.979
Wang and Singh	**a = -0.0032, b = 2.706×10^{-6}**	**2.99×10^{-4}**	**0.996**
Modified Page Equation II	c = 0.0051, L = -2.4025, n = 1.42515	4.22×10^{-4}	0.996
Drying temperature 70°C			
Model name	**Coefficients and constants**	**χ^2**	**R^2**
Lewis/Newton	k = 0.0123	3.420×10^{-3}	0.973
Page			0.832
Modified Page	k = 0.0116, n = 1.4450	6.78×10^{-4}	0.934
Henderson and Pabis	a = 1.0637, k = 0.0130	3.17×10^{-3}	0.975
Logarithmic	a = 1.1444, c = -0.1023, k = 0.0103	3.89×10^{-3}	0.985
Two-Term	a = 0.5318, b = 0.5338, k_0 = 0.0058, k_1 = 0.0073	2.29×10^{-3}	0.979
Approximation of Diffusion	a = 2.667×10^{-8}, k = 1.024×10^{-7}, m = 2.3793	4.39×10^{-3}	0.965
Wang and Singh	**a = -0.0087, b = 1.921×10^{-5}**	**2.59×10^{-4}**	**0.998**
Modified Page Equation II	c = 0.0017, L = 1.0246 , n = 1.4435	3.82×10^{-4}	0.928

Table 6.3 Values of model constants for thin-layer drying of culinary banana peel paste

Drying temperature 40°C			
Model name	**Coefficients and constants**	**χ^2**	**R^2**
Lewis/Newton	k = 0.0029	3.7×10^{-2}	0.9640
Page			0.9063
Modified Page	**k = 0.0028, n =1.4390**	**2.236×10^{-4}**	**0.9986**
Henderson and Pabis	a =1.1060, k = 0.0032	2.61×10^{-2}	0.9748
Logarithmic	a = 1.2293, c = -0.1735, k = 0.0022	8.659×10^{-4}	0.9917
Two-Term	a = 0.5530, b = 0.5530,m = 0.0032, n = 0.0032	2.842×10^{-2}	0.973
Approximation of Diffusion	$a = 5.47 \times 10^{-8}$, k = -53798.89, m =2.212	4.0×10^{-3}	0.9615
Wang and Singh	$a = -0.0021$ $b = 1.175 \times 10^{-6}$	3.431×10^{-4}	0.9967
Modified Page Equation II	c = 0.0146, m = -4.3223, n = 1.4354	2.815×10^{-4}	0.9947
Drying temperature 50°C			
Model name	**Coefficients and constants**	**χ^2**	**R^2**
Lewis/Newton	k = 0.0051	5.95×10^{-2}	0.9489
Page			0.9248
Modified Page	**k = 0.0049, n = 1.5612**	**2.654×10^{-4}**	**0.9982**
Henderson and Pabis	a = 1.1020, k = 0.0056	4.9×10^{-2}	0.9580
Logarithmic	a = 1.3291, c = -0.2825, k =0.0034	1.675×10^{-2}	0.9855
Two-Term	a = 0.5510, b = 0.5510, m = 0.0056, n = 0.0056	5.6×10^{-2}	0.9520
Approximation of Diffusion	a = -0.2020, k = 0.0304, m= 2.2683	3.8×10^{-3}	0.9667
Wang and Singh	$a = -0.0037$, $b = 3.421 \times 10^{-6}$,	9.929×10^{-4}	0.9914
Modified Page Equation II	c = 0.0049, m = -2.5886, n = 1.5567	7.10×10^{-4}	0.9939
Drying temperature 60°C			
Model name	**Coefficients and constants**	**χ^2**	**R^2**
Lewis/Newton	k = 0.0053	7.30×10^{-2}	0.9387
Page			0.9500
Modified Page	**k = 0.0051, n = 1.5781**	**2.657×10^{-4}**	**0.9966**
Henderson and Pabis	a = 1.1006, k = 0.0059	6.354×10^{-3}	0.947
Logarithmic	a = 1.4944, c =-0.45974, k = 0.0029	1.7×10^{-2}	0.9850
Two-Term	a = 0.5502, b = 0.8761, m = 0.0059, n = 0.0453	7.31×10^{-4}	0.9382
Approximation of Diffusion	$a = 1.262 \times 10^{-8}$, k = -426903.57, m = 2.1312	8.422×10^{-2}	0.9292
Wang and Singh	$a = -0.0037$, $b = 3.281 \times 10^{-6}$	1.38×10^{-3}	0.9885
Modified Page Equation II	c = 0.0051, m = -2.6155, n = 1.5730	1.7×10^{-2}	0.9856
Drying temperature 70° C			
Model name	**Coefficients and constants**	**χ^2**	**R^2**
Lewis/Newton	k = 0.0136	9.305×10^{-4}	0.9919
Page			0.8068
Modified Page	**k = 0.0131, n = 1.1895**	**2.642×10^{-4}**	**0.9977**
Henderson and Pabis	a = 1.0246, k = 0.0138	9.495×10^{-4}	0.9917
Logarithmic	a = 1.0659, c = -0.0553, k = 0.0120	4.435×10^{-4}	0.9961
Two-Term	a = 0.5123, b = 0.5123, m = 0.0138, n = 0.0138	1.272×10^{-3}	0.9890
Approximation of Diffusion	a = -0.1302, k = 0.1165, m = 3.0879	6.404×10^{-4}	0.9944
Wang and Singh	$a = -0.0093$, $b = 2.159 \times 10^{-5}$	8.991×10^{-4}	0.9922
Modified Page Equation II	c = 0.0032, m = 0.7797, n = 1.1841	3.026×10^{-4}	0.9973

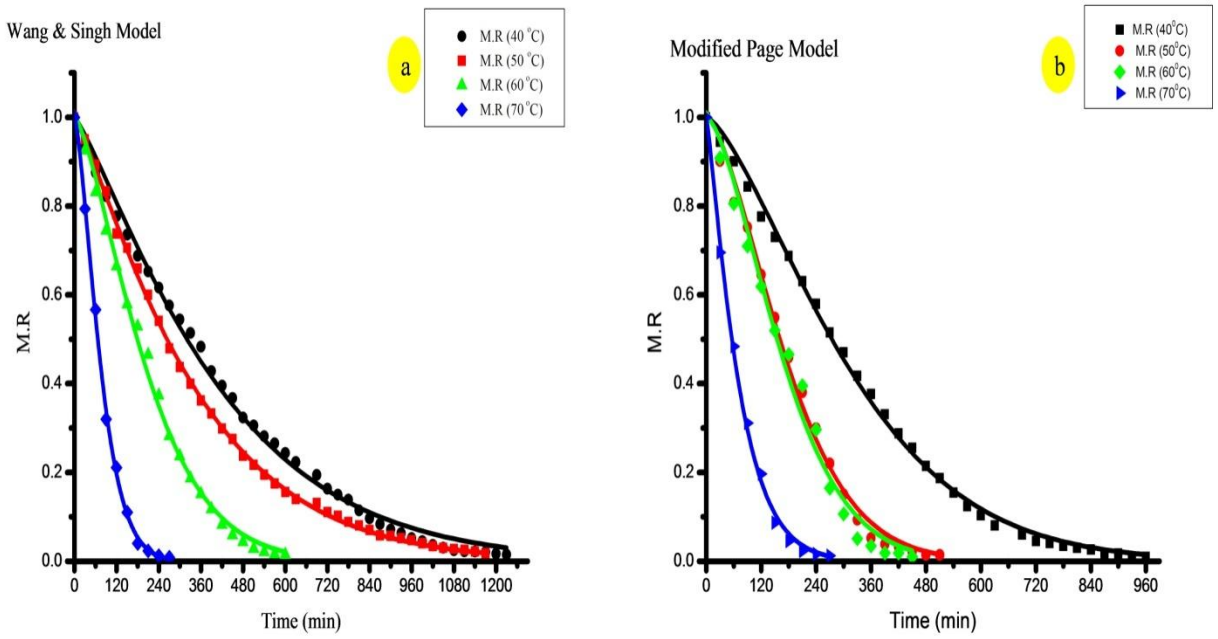

Fig 6.5 Moisture ratio vs drying time in **(a)** Wang & Singh model in pulp slices and **(b)** modified Page model peel paste

6.3.3 Effective moisture diffusivity

An analysis of the falling rate period was carried out to understand the drying kinetics and to determine the effective moisture diffusivity (D_{eff}) by slope method (Eq. 6.3). The relationship between ln MR with respect to time is illustrated in Fig. 6.6a (pulp) and Fig. 6.6b (peel) and the calculated values of D_{eff} for all the temperatures (40-70^{o}C) are shown in Table 6.4. The highest and lowest diffusivity (D_{eff}) values obtained in case of pulp slices was 8.38x10^{-9} m^2/s (at 70^{o}C) and 5.61x10^{-9} m^2/s (at 40^{o}C) respectively. Similarly, for peel, the highest diffusivity value of 7.80 x10^{-9} m^2/s was observed at 70^{o}C and the lowest D_{eff} value of 2.05 x10^{-9} m^2/s was observed at 40^{o}C. The results shows effect of temperature on effective moisture diffusivity which is useful for equipment design and scaling in the temperature range studied. The results revealed that D_{eff} increased with increase in temperature and are in line with Mitra et al.[33] in case of onion slices and Thuwapanichayanan et al.[22] in dessert banana slices dehydration. The obtained D_{eff} are also within the suitable range of various food products (10^{-11} to 10^{-9} m^2/s) as reported by a number of authors viz., cassava crackers,[34] bell-pepper,[35] sweet cherry[36] and ripe

banana slices.[22] Drying of most of the food materials occur in the falling rate period[37] and moisture transfer during drying is controlled by internal diffusion.[38] From the study it can be concluded that effective moisture diffusivity declined sharply with moisture content in the first falling rate period and when drying entered into the second falling rate period the diffusivity changed slightly with moisture content.

Table 6.4 Effective moisture diffusivity, activation energy of culinary banana

Temp (^oC)	D_{eff} (m^2/s)		ln (D_{eff})		$1/T_{abs}$	
	Pulp slices	Peel paste	Pulp slices	Peel paste	Pulp slices	Peel paste
40	$5.6X10^{-9}$	$2.05 x10^{-9}$	-19.0005	-20.0054	0.00319	0.003195
50	$6.6X10^{-9}$	$3.85 x 10^{-9}$	-18.8361	-19.375	0.00309	0.003096
60	$7.24X10^{-9}$	$4.05 x 10^{-9}$	-18.7436	-19.3245	0.00300	0.003003
70	$8.38X10^{-9}$	$7.80 x 10^{-9}$	-18.5974	-18.669	0.00291	0.002915

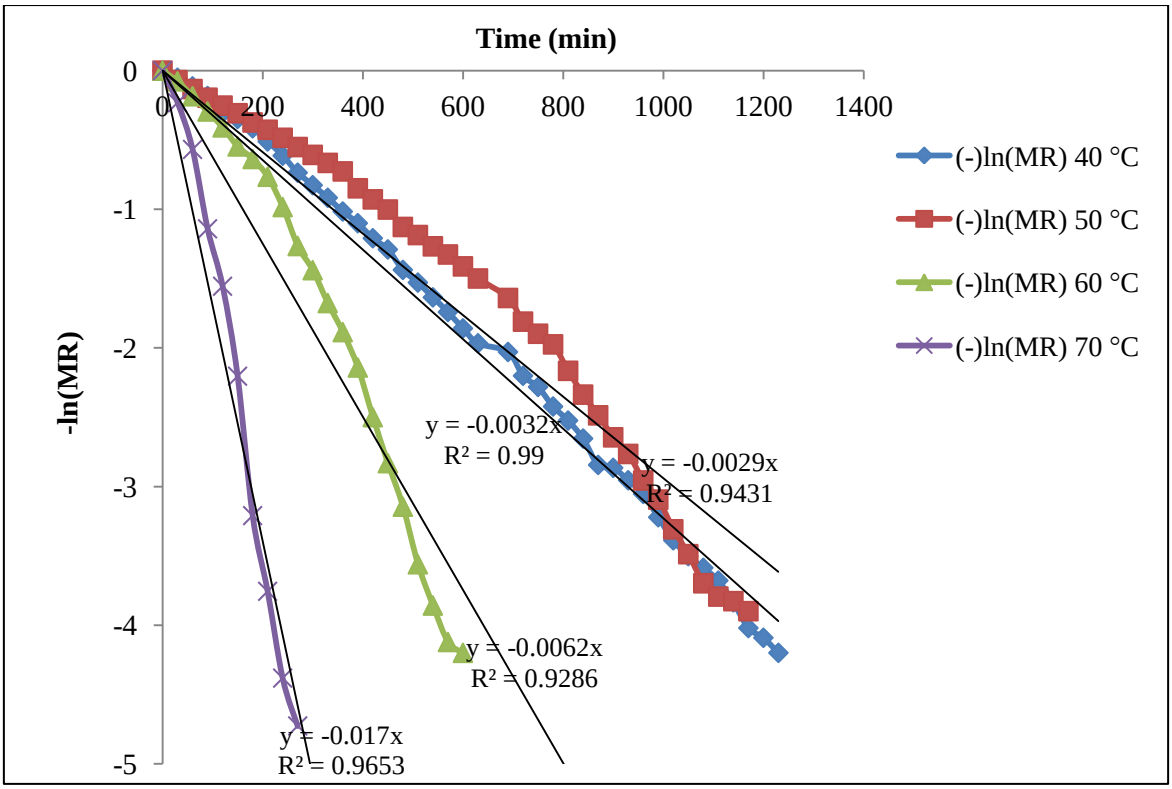

Fig. 6.6a Variation in ln (MR) with time (t) of pulp slices

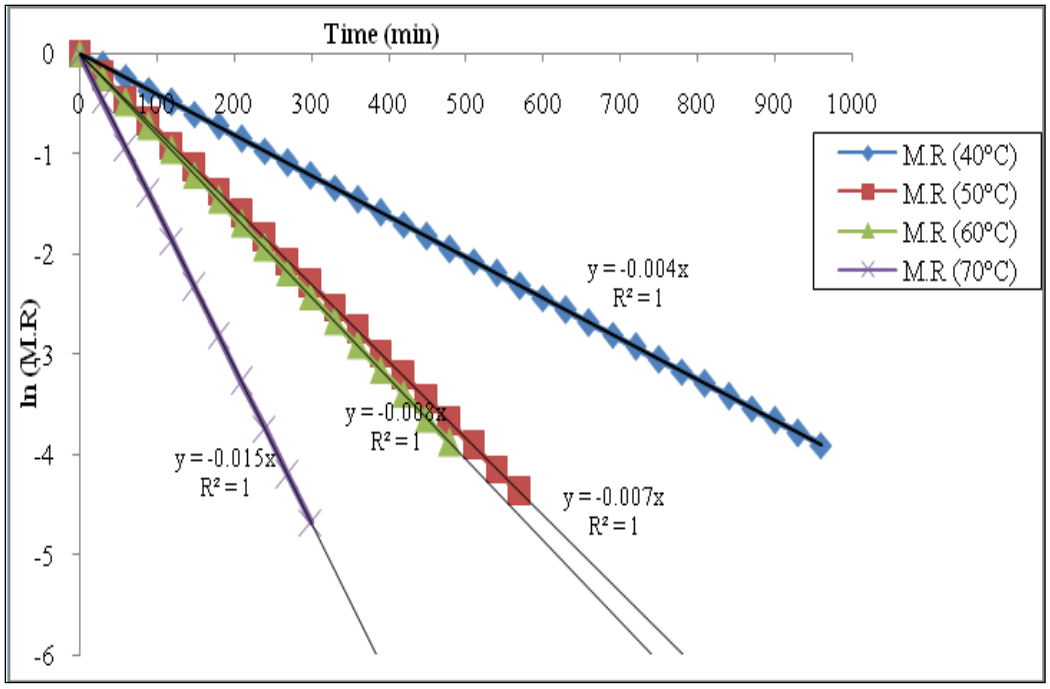

Fig. 6.6b Variation in ln (MR) with time (t) of peel paste

6.3.4 Activation energy

Activation energy is the minimum energy required to initiate moisture diffusion from the food products. The ln D_{eff} versus function of the inverse of absolute temperature (in K) was used to obtain the constants of Arrhenius equation (Table 6.5; Fig. 6.7a and 6.7b). The plots in Figs. 6.7a and 6.7b were found to be a straight line (linear relationship) between (ln D_{eff}) and (1/T) in the temperature range investigated, indicating the Arrhenius type relationship with R^2 values of 0.89 and 0.99 for pulp and peel respectively. Using Eq. (6.5) the activation energy was calculated and found 53.27 and 27.22 kJ/mol for pulp and peel respectively. The results can be corroborated with the findings of several authors viz., Zogzaz et al.[39] for most food materials (12.7 to 110 kJ/mol) Doymaz[11, 40] in fruits and vegetables (23.44- 51.08 kJ/mol), tomato (32.94 kJ/mol) and in green peas (51.26 kJ/mol).

Table 6.5 Progressive parameters of Arrhenius relationship between effective diffusivity and absolute temperature

Regression parameters	Values	
	Pulp slices	Peel paste
Slope (E_a/R)	-6414	327.48
Activation energy (E_a)	53.27 kJ/mol	27.22 kJ/mol
Intercept (ln D_o)	1.25	8.9 x 10^{-2}
R^2	0.89	0.99

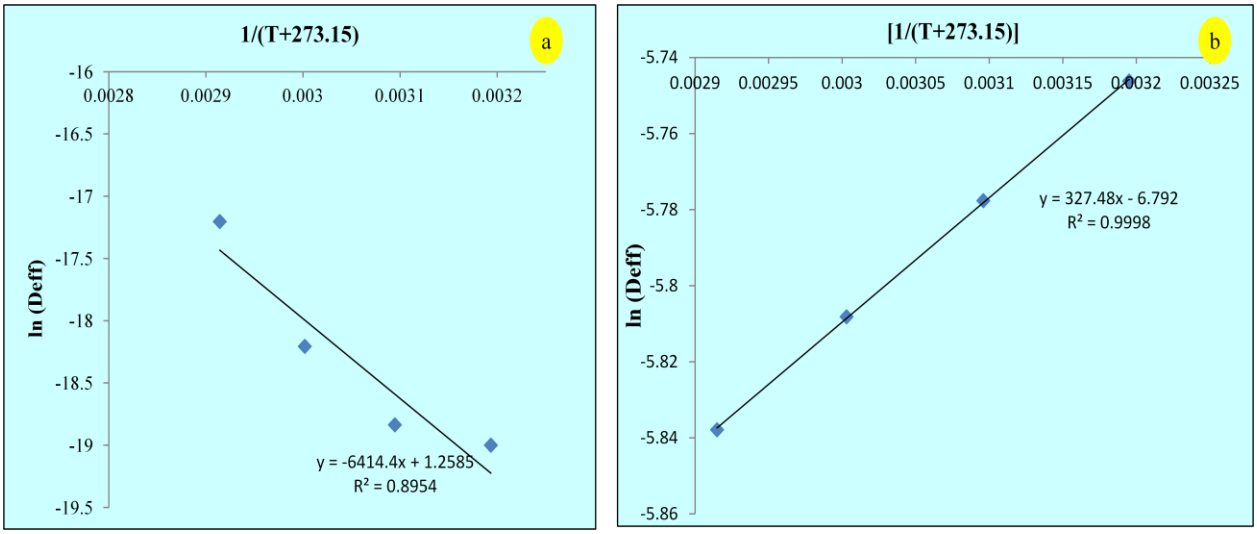

Fig. 6.7 Logarithmic of effective moisture diffusivity vs function of the inverse of absolute temperature (K) of **(a)** pulp slices and **(b)** peel paste

6.3.5 Physicochemical analysis

6.3.5.1 Microstructure evaluation

Scanning electron microscopic (SEM) studies of culinary banana samples dried at various temperatures are illustrated in Fig. 6.8 (pulp) and Fig. 6.9 (peel). The effect of drying temperatures (40-70^{o}C) on the microstructure of culinary banana was characterized by small or large pores. As shown in both the Figs. 6.8 and 6.9, samples dried at 40^{o}C created large number of smaller size pores and led to the dense structure of the final dried product. The pore formation

in dried sample is due to the evaporation of water vapour from the cells which led to the development of internal pressure and breakage of the sample tissues, resulting in the formation of pores.[31] Abbasi et al.[41] also reported that low temperature long time heating causes stress in the cellular structure of food which leads to the denser structure with large number of smaller size pores which are in line with the current findings. On the other hand, the number of pore size increased with increase in drying temperature as shown in figures. Results revealed that when samples were dried at 70^{o}C, highly porous final product was obtained with larger pore size. From the result it can be concluded that drying at higher temperature may raise the hydrostatic pressure gradient of moisture between inside and outside of the dried samples which subsequently leads to large pores and voids.[42] These pores and void space not only affect the textural property, but also the transport properties such as diffusivities of gases and liquids in the sample resulting in higher rate of effective moisture diffusivity at higher temperature drying[31] which corroborate our results.

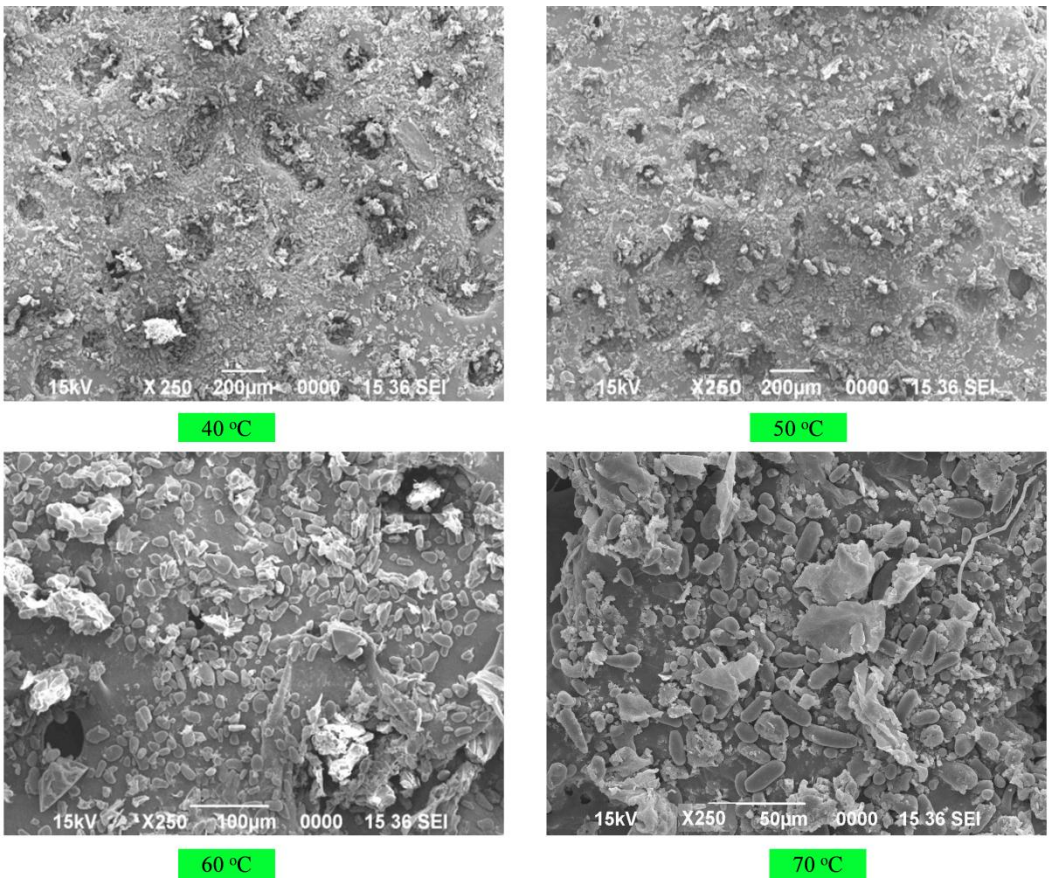

Fig. 6.8 Scanning electron micrographs of pulp dried at various temperatures

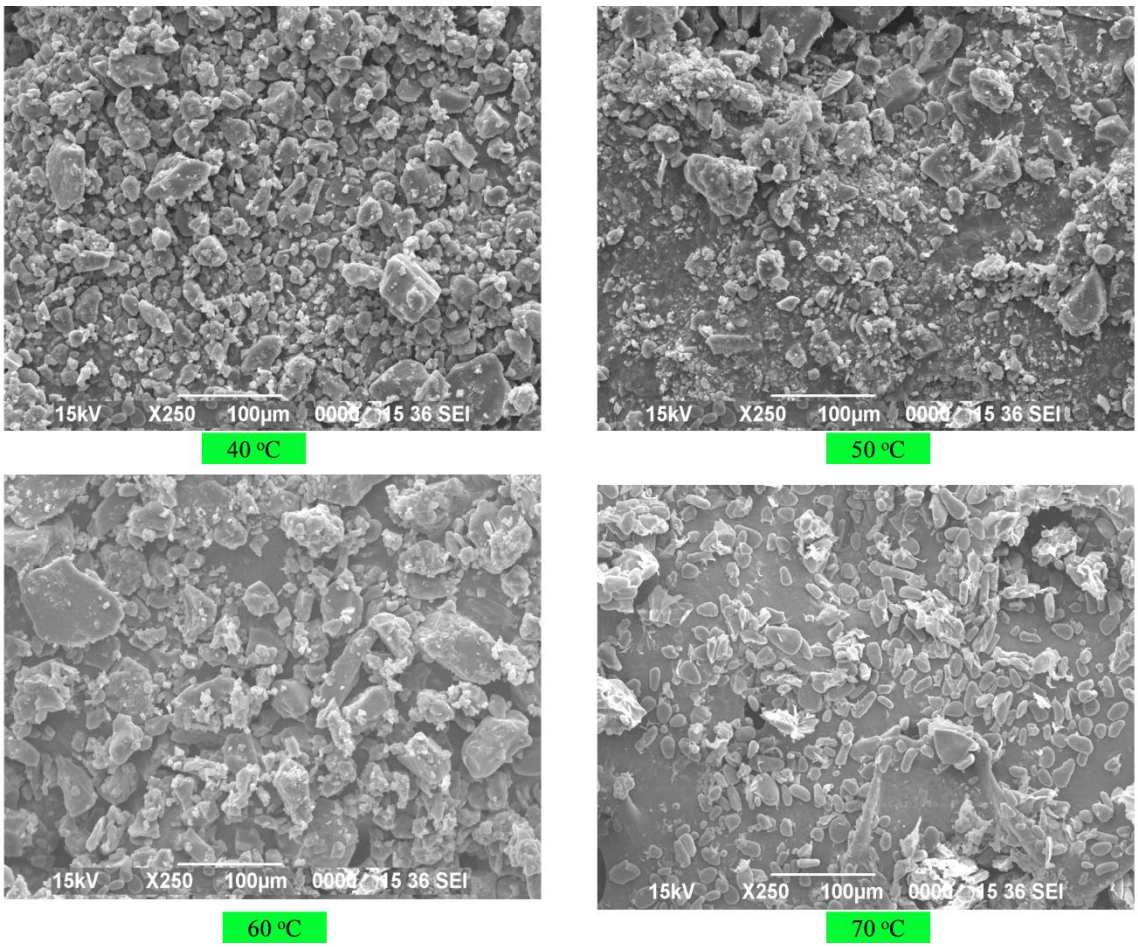

Fig. 6.9 Scanning electron micrographs of peel dried at various temperatures

6.3.5.2 Textural property

Textural property was evaluated only in pulp as it was in flakes form, the peel was dried in a paste form which was further ground into powder, therefore, textural properties of only pulp was studied. Dried culinary banana slices are affected by various drying temperatures and are strongly associated with composition and structure of cell walls (Table 6.6). The hardness or crispness may be attributed to the intermolecular bonding of starch and forming small crystalline like regions when small amount of water is present in the sample. Samples dried at 70^{o}C required lowest maximum forces to obtain the force deformation curve and reverse is the case at 40^{o}C dried samples. The result revealed that texture of dried banana slices in terms of hardness is found maximum in samples dried at lower temperature which had reduced rehydration rate and capacity and are in agreement with various authors.[43, 44] On the contrary, samples dried at higher

temperature (70^{o}C) possess large porous structure which required lowest maximum force,[22] and in addition, drying at higher temperature leads to more volume and a crust on the surface of the product giving better reconstitution properties.[45]

6.3.5.3 Nonenzymatic browning

Nonenzymatic browning of dried culinary banana was measured using Eq. (6.6) in terms of optical index as presented in Table 6.6 and Table 6.7 for pulp and peel respectively, and revealed that it occurred faster at higher temperature (70^{o}C) in both dried samples compared to lower temperature (40^{o}C) and was statistically different. The samples dried at 70^{o}C showed major browning values and may be due to Millard reaction as well as ascorbic acid oxidation at higher temperature.[46] Manuel and Sereno[47] reported the increase in non-enzymatic browning in onion and strawberry with respect to time.

6.3.5.4 Rehydration ratio

The rehydration capacity of dehydrated banana slices (Table 6.6) and peel (Table 6.7) were obtained using Eq. (6.7). The rehydration ratio of pulp was in the range of 2.84-7.83 and in case of peel it was recorded in the range 5.48-8.76 and they varied significantly. The rehydration ratio of peel was higher compared to pulp, this is because the pulp was in a flake form and peel was in a power form, hence, it was easier for peel powders to rehydrate easily than pulp slices. However, in both the cases, rehydration ratio at higher temperature was better over the lower temperature. Less damage occurred to the pore structure when samples were subjected to faster drying at higher temperature while prolonged heating at lower temperature causes greater shrinkage which lowered the rehydration ratio and results are in agreement with Mitra et al.[33] According to the study of Orikasa et al.[48] the surface hardening of samples during prolong drying process caused decreasing moisture diffusion which might be also one of the reasons for minimum rehydration ratio of low temperature dried samples.

6.3.5.5 Determination of DPPH radical scavenging activity and total polyphenols

The DPPH radical scavenging activity of dried pulp samples was found in the range of 47.49 - 50.52 % SA (Table 6.6) and in case of peel it was in the range of 78.48-86.53 % (Table 6.7). The result revealed that the drying temperature (40-70^{o}C) and scavenging activity significantly varied with respect to dying temperature. Total polyphenols content of dried culinary banana was in the range of 166.32-176.75 mgGAE/100g in pulp and 987.96-1037.87 mgGAE/100g in peel. With increase in drying temperature, both antioxidant activity and polyphenols decreased significantly. Decrease in antioxidant activity at higher drying temperature is also reported by Ozgur et al.[49]

Table 6.6 Texture, rehydration ratio (RR), non-enzymatic browning (NEB), DPPH scavenging activity (SA) and total phenolic content (TPC) of dried culinary banana pulp

Temp (^{o}C)	Maximum force (N)	NEB (OI/g)	% RR	DPPH SA (%)	TPC (mgGAE/100g)
40	56.69±4.89^{d}	28.64±2.36^{a}	2.84±0.96^{a}	50.52±1.05^{d}	176.75±1.90^{d}
50	49.37±3.76^{c}	31.53±1.78^{b}	4.63±0.66^{b}	49.53±1.80^{c}	174.86±1.33^{c}
60	38.94±4.42^{b}	33.84±2.91^{c}	6.73±0.95^{c}	48.56±1.62^{b}	168.68±1.17^{a}
70	30.33±2.41^{a}	36.78±2.42^{d}	7.83±1.04^{d}	47.49±1.77^{a}	166.32±1.24^{b}

^{a}Mean in columns followed by the same letters are not significantly different at p>0.05; values represent mean±SD, n=3

Table 6.7 Rehydration ratio (RR), non-enzymatic browning (NEB), DPPH scavenging activity (SA) and total phenolic content (TPC) of dried peel

Temp (^{o}C)	NEB (OI/g)	% RR	DPPH SA (%)	TPC (mgGAE/100g)
40	36.54±0.97^{a}	5.48±0.02^{a}	86.53±1.24^{d}	1037.87±4.23^{d}
50	39.67±1.08^{b}	6.23±0.07^{b}	83.47±0.97^{c}	1026.50±3.27^{c}
60	44.53±0.86^{c}	7.15±0.12^{c}	81.39±0.68 ^{b}	1006.24±4.55^{b}
70	48.91±0.94^{d}	8.76±0.03^{d}	78.48±1.11 ^{a}	987.96±4.78^{a}

^{a}Mean in columns followed by the same letters are not significantly different at p>0.05; values represent mean±SD, n=3

6.4 Conclusions

Among the nine different drying kinetic models, Wang and Singh in case of pulp and modified Page in case of peel was the most suitable models having highest R^2 and lowest χ^2 values. The effective moisture diffusivity (D_{eff}) increased with increase in drying temperature. Assessment of various quality attributes in dried culinary banana pulp and peel revealed that temperatures significantly affected the texture, rehydration ratio, nonenzymatic browning and microstructure. However, antioxidant activity and total polyphenols significantly decreased with increase in drying temperatures. SEM images evinced that samples dried at higher temperature had larger pores and better rehydration ratio compared to lower temperature dried samples. The structure of food can have a profound influence on quality attributes and nutritional value. Drying at lower temperature yielded better results for colour whereas higher temperature gave better textural property, rehydration ratio and microstructure of the dried products. Hence, this study provides information on thin layer dehydration characteristics of culinary banana at varying temperatures. The information found in this research can be useful in the design, simulation of drying equipment, and the exploitation of culinary banana as a source to obtain many nutritionally rice value added products like bread, noodles, pasta, cookies etc.

B) Modeling and optimization of the process parameters in vacuum drying of culinary banana pulp slices and peel paste

6.5 Introduction

Drying of fruits and vegetables is an economically important process to prolong shelf life and to provide convenience to the consumer.[50] Currently air drying is dominating technology due to cost effectiveness, but product quality in terms of appearance, texture, nutrients etc is comparatively conciliated.[51] Freeze drying yields high quality products but at larger operational cost is not economic for fruits and vegetables.[1] The most important thing in the food industry nowadays is to produce high quality product with increased productivity and reduced production cost.[52] Therefore looking at the backdrop of various dehydration techniques, vacuum drying is a novel alternative method of drying in terms of cost as well as quality product. According to the study of Das[53] in vacuum drying process removal of moisture from food takes place at sub-atmospheric pressure. The food samples kept on heated plate inside the vacuum dryer supplies latent heat required for evaporation of water from food. Vacuum in the range of 10 and 50 mm of Hg absolute pressure is maintained inside the dryer and this pressure corresponds to saturation temperature of water between 11 and 38^{o}C. As, temperature of heated plate is higher than the saturation temperature of water, pure water will boil inside the dryer and food samples can be completely dried.[53] The mechanism of vacuum drying takes place by removing moisture from food under low pressure is also reported by Jaya and Das.[54] A thin layer of food is placed on a heated plate which supplies latent heat requires for evaporation water from the food and the drying takes place in absence of oxygen, oxidative degradation.

One of the most important stages of drying technology is modeling and optimization of the process to increase the efficiency of the drying facilities and quality of the product. In drying processes, complex and highly nonlinear phenomena are involved.[55] The construction of relationship between the physical properties and structure of dried foods, such as models based on theoretical constructs, regression analysis, or principal component analysis several methods are there. Depending on the type of product, moisture content, drying type and drying conditions the properties of dried foods vary substantially. Therefore, drying modeling is key important for the optimization of operating parameters and performance improvements of the drying system.[56]

Thus, a promising approach is to use artificial neural network (ANN) analysis which has been recognized as a powerful tool particularly for the case of nonlinear and multiple processing systems.[57] ANNs have high learning ability and capability of identifying and modeling the complex non-linear relationships between the input and output of a system with an appropriate choice of free parameters or weights.[58, 59] ANN has been used by various researchers to describe the drying characteristics of many agricultural products like mango ginger,[60] carrots,[61] tomato,[62] and *Echinacea angustifolia*.[63]

On the other hand, genetic algorithm (GA) is one of the search methods and optimization techniques which aim at an optimal value of a complex objective function by simulating biological evolutionary processes based on genetics (crossover and mutation).[63] As stated by Mohebbi et al.[64] GA is inspired by the natural selection principles and Darwin's species evolution theory. GA offers several advantages over the conventional optimization method such as less susceptibility to be stuck at local minima, requiring little knowledge of the process being optimized and capability to find the optimum conditions when the search space is very large.[65] The principles of GA are based on natural competitions of beings for appropriating limited natural sources.[64] Because of its robustness and easy customization for different kinds of optimization problems, GA has widely been applied in food engineering. In preliminary studies drying characteristics of both pulp and peel were conducted. The aim of this present study is to optimize the process parameters of vacuum drying of culinary banana pulp slices and peel by using ANN and GA by studying the effect of different drying conditions on its physical and chemical properties.

6.6 Materials and methods

6.6.1 Sample preparation

Fresh culinary bananas were harvested from Tezpur University campus. The samples were then thoroughly cleaned and peeled. The initial moisture content of sample was measured by vacuum oven drying method as described by Rangana.[6] The fresh and dry weights were measured with an electronic weighing balance (CPA225D, Sartorius AG, Germany) having 0.001g accuracy.

6.6.2 Experimental design

The most predominant parameters governing the vacuum drying of culinary banana are drying temperature (X_1), sample slice thickness (X_2) and pretreatment (X_3). It was desired to find the effect of these three independent variables on the quality of finally obtained product. The quality of the product was evaluated in terms of four responses i.e. rehydration ratio (Y_{RR}), scavenging activity (Y_{SA}), nonenzymatic browning (Y_{NEB}) and hardness (Y_H). The selection of level extremes (X_{max} and X_{min}) was fixed on the basis of literature survey[33] and preliminary experiments. The temperature level used for drying the samples was in the range of 40 to 80^oC which varied at 5 levels i.e. 40, 50, 60, 70 and 80^oC. The thickness of both samples was maintained in the range of 2-8 mm and varied at 4 levels (2, 4, 6 and 8 mm). To deactivate the enzymatic browning of samples during drying, the samples were pretreated with different concentrations of citric acid solution for 15 min prior to drying. To obtain the effect of pretreatment on product quality, it was varied at 4 levels and untreated sample was taken as a control. Hence the level of pretreatment was kept as 0, 0.5, 1 and 1.5% of citric acid out of which 0% indicates control sample. The total runs of 80 experiments for each sample (pulp and peel) were obtained in accordance to general factorial design (5x4x4). The experiments were conducted and all the responses were measured to optimize the process parameters during vacuum drying of culinary banana slices. Design Expert Version 7 (Stat-Ease, Inc.) was used to design the experiments.

6.6.3 Experimental procedure

The samples were peeled and inner core of fruit was sliced manually into the specified thickness as obtained from the experimental design. Manual self designed slicer (Fig. 6.2) was used to slice the pulp samples with a uniform thickness. In case of peel paste, the thickness of paste was maintained in Petri plates. The vacuum drying of samples was carried out inside a laboratory scale vacuum dryer (K-VO64, K&K Scientific Supplier, South Korea). A constant 50 mm Hg absolute pressure level (710 mm Hg vacuum) was maintained[33] at five different plate temperatures of 40, 50, 60, 70 and 80^oC. Once the steady state condition was achieved inside the vacuum drying chamber, the trays loaded with sample were placed inside the drying chamber.

The experiment was continued until the sample attained constant weight. Each experiment was conducted thrice and average values of all the responses were taken for further analysis.

6.6.4 Quality evaluation

The quality parameters studied were structural morphology by SEM (method described in section 6.2.5.1), texture analysis (method described in section 6.2.5.2), non enzymatic browning (method described in section 6.2.5.3), rehydration ratio (method described in section 6.2.5.4), radical scavenging activity (method described in section 2.2.2.5).

6.6.5 Response surface methodology

In order to achieve the relationship between three input factors viz., temperature (X_1), slice thickness (X_2) and pretreatment(X_3) vis-a-vis four responses studied i.e. rehydration ratio (Y_{RR}), scavenging activity (Y_{SA}), nonenzymatic browning (Y_{NEB}) and hardness (Y_H) the runs were designed using RSM. Second order polynomial model was fitted to the data and to relate these responses (Y_{RR}, Y_{SA}, Y_{NEB}, Y_H) four models in the form of Eq. (6.8) were developed.

$$Y_k = \beta_{k0} + \sum_{i=1}^{4} \beta_{ki} x_i + \sum_{i=1}^{4} \beta_{kii} x_i^2 + \sum_{i=1}^{3} \sum_{j=i+1}^{4} \beta_{kij} x_i x_j \qquad \text{Eq. (6.8)}$$

Where β_{k0}, β_{ki}, β_{kii} and β_{kij} are constant regression coefficients and x is the coded independent variables. Mathematical models were evaluated by means of multiple regression analysis. By using the Box-Cox plot the variables of the responses were transformed to make the distribution closer to the normal distribution and improving the model fit to the data.[66] Model adequacies were checked by R^2 and coefficient of variation (CV%) by using Eq. (6.9) and (6.10) respectively (Myers).[67]

$$R^2 = 1 - \frac{\sum_{i=1}^{N}(yi - ydi)^2}{\sum_{i=1}^{N}(ydi - ym)^2} \qquad \text{Eq. (6.9)}$$

Where N= no of data, *yi* = predicted values by ANN model, *ydi* = actual or experimental values, *ym* = average of actual values

The CV% was calculated as

$$C.V\ \% = \frac{Std.Dev}{Mean} \times 100 \qquad \text{Eq. (6.10)}$$

6.6.6 Artificial neural network (ANN) development and coding

The schematic diagram of ANN employed in the present study for predicting relationship between independent and dependent parameters are given in Fig. 6.10. The figure illustrates three input layers for the independent variables, five hidden layers and four output layers representing the responses. ANN was simulated based on a feed forward back propagation (FFBP) neural network using MATLAB (MathWorks R2012b, US). The procedure used to calibrate the ANN model was "training" or "learning" which seeks the optimal weight. The coding of input data set (X_1, X_2, X_3) was done for developing the ANN model which lies within the range of -1 and +1. The output data set (Y_{RR}, Y_{SA}, Y_{NEB}, Y_H) was coded in the range of 0 and +1.

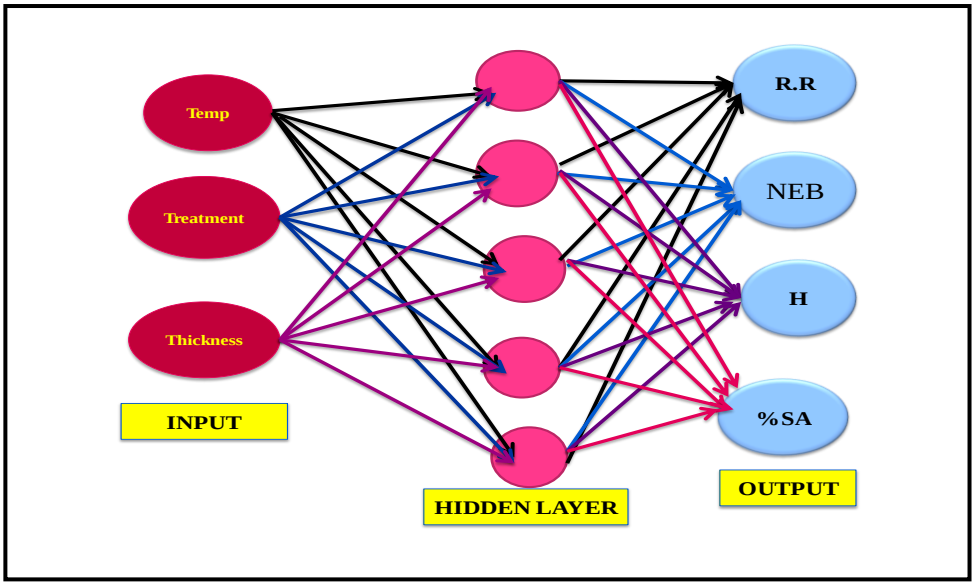

Fig. 6.10 Schematic diagram of MLFF ANN

In the present study, 'nx =3' is considered as the number of independent variables or input (coding of the parameters lies in the range of -1 and +1). The number of dependent variables represented as 'ny = 4' (coding of the parameters lies in the range of 0 and +1). A single output data series is mathematically represented by a row matrix 'y' of size (ny*1 = 4*1). Out of 'n' sets of input-output data, only one set of data was utilized at a given time. Therefore, a single

input and output datasets are represented by a row matrices 'x' and 'y' of sizes (nx*1 = 3*1) and (ny*1 = 4*1) respectively. The weight of synaptic joints between the input and hidden layer neurons have been designated by matrix 'u' and its size is represented as nx*nh = 3*5. Here, 'nh = 5' is the number of hidden layers considered for the ANN study. The weight of synaptic joint 'w' between hidden and output neuron layer has a size of 5*4 (nh*ny = 5*4). The bias or threshold values of the hidden layer neuron 'Th' is the vector or column matrix of size "nh*1" and the obtained value for the present case is 5*1. 'To' the bias or threshold values of the output layer neuron is the vector or column matrix of size 4*1 (ny*1 = 4*1). The element of matrix 'u', 'w', 'Th' and 'To' were generated by random number generation and their values were between -1 and +1.

Similarly, 'yh' and 'yo' are computed output values of hidden and output layer neurons respectively which are expressed in Eq. (6.11) and (6.12).

$$yh = \frac{1}{1+\exp\left[-(u' * x' + Th)\right]} \quad \text{Eq. (6.11)}$$

$$yo = \frac{1}{1+\exp[-(w' * yh + To)]} \quad \text{Eq. (6.12)}$$

Where $u'$and x' are the transpose of matrix 'u' and 'x' and the size of matrix 'yh' and 'yo' are nh*1 and ny*1 which are equal to 5*1 and 4*1 respectively.

Now 'eo' and 'eh' are back propagation error at hidden and output layer neurons respectively which are used for updating the values of 'u', 'w', 'Th' and 'To' in the next computation cycle. The computed value of error 'eo' at the output layer was calculated using Eq. (6.13).

$$eo = (y' - yo)_o * yo_o * (w' * eo) \quad \text{Eq. (6.13)}$$

Where '*eo*' is the scalar product of matrices $(y' - yo)$, 'yo' and (1-yo) and *y'* is the transpose of the matrix 'y'. The size of the matrix 'eo' is represented as ny*1 = 4*1.

The computed value of error 'eh' at the hidden layer neuron is expressed in Eq. (6.14).

$$eh = yh_o * (1 - yh)_o * (w * eo) \quad \text{Eq. (6.14)}$$

In the above equation 'yh' and (1-yh) form scalar product and (w*eo) forms a vector product and the size of matrix 'eh' is (nh*1 = 5*1). To start with the ANN calculation, the values of first set

of input data 'x' and output data 'y', and the assumed values of matrices 'u', 'w', 'Th' and 'To' were used to obtain the values of 'yh', 'yo', 'eo' and 'eh' by using the above equations (Eq. 6.11 to 6.14).

Similarly, for the next computation cycle the new values of the bias or threshold parameter 'To_{new}' of output layer neurons, 'Th_{new}' of hidden layer neurons, 'u_{new}' of lines joining input and hidden layer neuron and 'w_{new}' of lines joining hidden and output layer neurons were obtained using Eq. (6.15) to Eq. (6.18)

$$To_{new} = L * eo + To \quad \text{Eq. (6.15)}$$

$$Th_{new} = L * eh + Th \quad \text{Eq. (6.16)}$$

$$u_{new} = x' * L * eh' + u \quad \text{Eq. (6.17)}$$

$$w_{new} = L * yh * eo' + w \quad \text{Eq. (6.18)}$$

Where 'L' is the learning rate and its value lies in the range between 0.6 and 0.9. The new values of 'u', 'w', 'Th' and 'To' were calculated as 'u_{new}''w_{new}', 'Th_{new}' and 'To_{new}' respectively by taking the value of learning rate parameter 'L' as 0.6. These obtained new values were used for second set of input-output data pairs which was again used for the third set of input-output data pairs and so on. The computations were continued in cyclic manner till the relative deviation percentage between the actual and estimated values of dependent variables was minimum. All the input-output data pairs (experimental) were carried out by single computational cycle and after completing the large number of computational cycle the final values of "u", 'w', 'Th' and 'To' yielded the final values of 'yo' for all the input data sets. The value of 'yo' is the coded value of the responses and lies between 0 and +1. The obtained coded values of the responses were converted to their corresponding real values. Finally, the ANN model adequacies were validated by estimation of the mean relative deviation percentage.

$$R_d = \frac{MD}{MV} X100 \quad \text{Eq. (6.19)}$$

Where, MD is the mean deviation and MV is the mean value.

6.6.7 Genetic algorithm (GA) as an optimizing tool for process parameters

Once an ANN based model with good prediction accuracy is fitted, GA could be used to optimize its input space representing the medium (Fig. 6.11). The GA based search begins with a population of representing random solutions. GA optimization method consists of four steps viz., selection, reproduction, crossover, and mutation.[68] For this purpose, the initial population of chromosomes is randomly generated. Selection of individuals to produce successive generations plays an extremely important role in a GA. In this step, each chromosome is evaluated by the fitness function. According to the value of the fitness function, the chromosomes associated with the fittest individuals are selected more often than those associated with unfit ones.

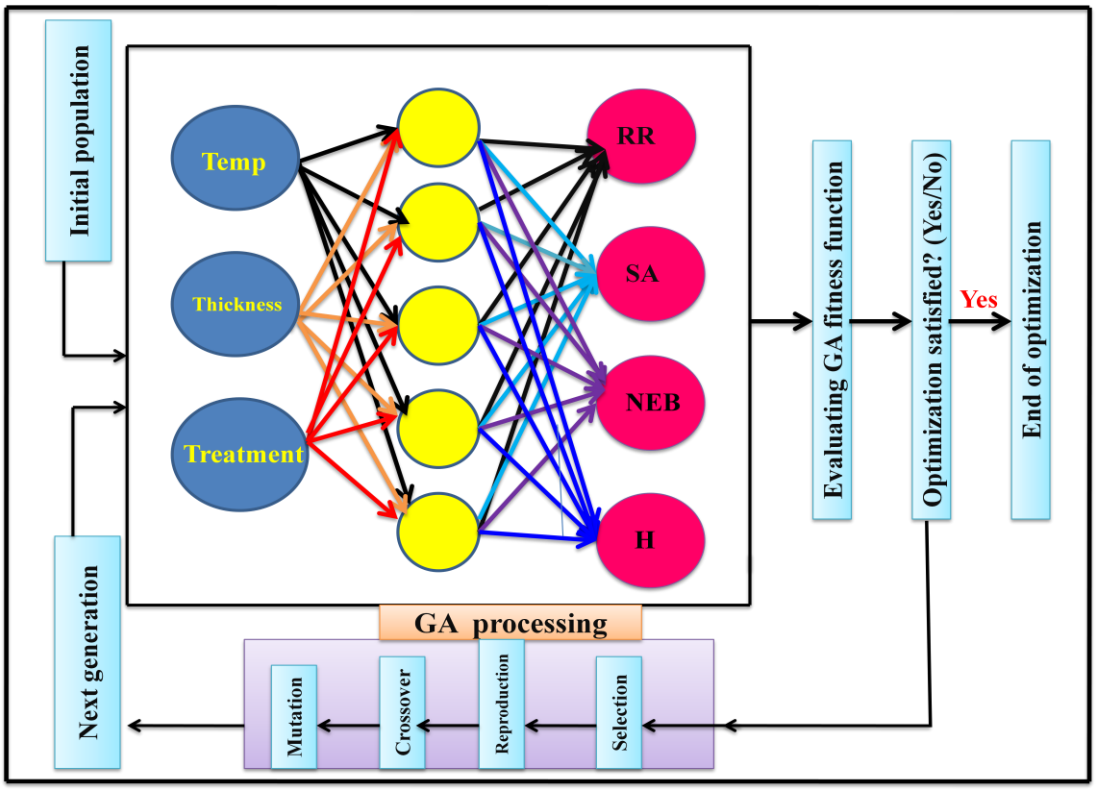

Fig. 6.11 Schematic diagram of optimization process of neural network using genetic algorithm

In the present case the fitness function was formulated based on maximization of rehydration ratio and scavenging activity and minimization of nonenzymatic browning and hardness and hence the fitness function is formulated as

$$F = Y_{RR} + Y_{SA} + \frac{1}{(1+Y_{NEB})} + \frac{1}{(1+Y_H)}$$ Eq. (6.20)

In crossover step, two individuals (parents) reproduced into a new individual. The mutation operation consists of randomly altering the value of each element of the chromosome according to the mutation probability. It provides the means for introducing new information into the population. This cycle is repeated until desired convergence on optimal or near-optimal of the solutions are achieved. In the present work, number of hidden neurons and training parameters will be represented by haploid chromosomes consisting of three genes of binary numbers. The first gene corresponds to the number of neurons in single hidden layer and second and third genes represent the learning rate and momentum of network respectively. In this process after mutation the population was operated again for the reproduction, crossover and mutation in the next cycle. The process is continued until the sum of square of the error between the mean and individual fitness value of the strings comes out to a very low value.

6.7 Results and discussion

6.7.1 Modeling of the process parameters by response surface methodology

Altogether 80 experiments each for pulp and peel were performed to examine the combined effect of drying temperature (X_1), sample slice thickness (X_2) and pretreatment (X_3) (independent variables) on rehydration ratio (Y_{RR}), scavenging activity (Y_{SA}), nonenzymatic browning (Y_{NEB}) and hardness (Y_H) (responses) in vacuum dried banana. Multiple linear regression analysis of the experimental data yielded second order polynomial models for prediction. The final equation obtained in terms of coded factors for four responses in case of pulp samples are presented as:

$$Y_{RR} = 4.362 + 1.003x_1 + 0.558x_2 + 0.543x_3 + 0.072x_1x_2 + 0.365x_1x_3 + 0.001x_2x_3 + 1.60x10^{-16}x_1^2 + 3.25x10^{-16}x_2^2 + 0.134x_3^2$$ Eq. (6.21)

$$Y_{SA} = 46.722 - 4.202x_1 - 2.523x_2 + 2.324x_3 + 1.036x_1x_2 - 0.026x_1x_3 + 0.999x_2x_3 + 2.24x10^{-15}x_1^2 + 2.26x10^{-15}x_2^2 - 0.771x_3^2$$ Eq. (6.22)

$$Y_{NEB} = 27.563 + 1.588x_1 + 1.703x_2 - 3.373x_3 + 0.428x_1x_2 + 0.435x_1x_3 + 1.198x_2x_3 + 1.44x10^{-15}x_1^2 + 1.43x10^{-15}x_2^2 - 0.682x_3^2 \quad \text{Eq. (6.23)}$$

$$Y_H = 47.216 - 92x_1 - 47.893x_2 - 14.893x_3 - 0.571x_1x_2 + 15.214x_1x_3 + 4.772x_2x_3 + 1.23x10^{-13}x_1^2 + 2.85x10^{-13}x_2^2 - 9.459x_3^2 \quad \text{Eq. (6.24)}$$

Similarly, for peel samples, equation obtained in terms of coded factors for three responses are presented in equations (6.25-6.27)

$$Y_{RR} = 6.763 + 1.541x_1 + 1.235x_2 + 1.396x_3 + 0.328x_1x_2 + 0.986x_1x_3 + 0.029x_2x_3 + 1.42x10^{-12}x_1^2 + 3.23x10^{-11}x_2^2 + 1.281x_3^2 \quad \text{Eq. (6.25)}$$

$$Y_{SA} = 84.283 - 5.392x_1 - 4.062x_2 + 1.841x_3 + 1.128x_2 - 1.529x_1x_3 + 2.093x_2x_3 + 1.283x10^{-16}x_1^2 + 3.191x10^{-14}x_2^2 - 1.209x_3^2 \quad \text{Eq. (6.26)}$$

$$Y_{NEB} = 33.761 + 1.082x_1 + 2.067x_2 - 4.873x_3 + 1.672x_1x_2 + 1.708x_1x_3 + 2.057x_2x_3 + 1.76x10^{-15}x_1^2 + 2.18x10^{-15}x_2^2 - 1.293x_3^2 \quad \text{Eq. (6.27)}$$

Model adequacies were checked by R^2 and coefficient of variation (CV%) are presented in Table 6.8. The R^2 values pulp for rehydration ratio, scavenging activity, nonenzymatic browning and hardness were found to be 0.90, 0.78, 0.89 and 0.97 respectively. The obtained R^2 values are in reasonable agreement with the adj-R^2 and predicted R^2 values (Table 6.8) showing thereby to fulfill the goodness of the model fit. The adequate precision for the models Y_{RR}, Y_{SA}, Y_{NEB}, and Y_H were 27.57, 14.68, 19.76 and 54.77 respectively. In all the cases the adequate precision value (signal to noise ratio) of the models were found to be greater than 4 demonstrating the adequate signal. This signifies that the model can be used to navigate the designed space. The CV% indicated the relative dispersion of the experimental points from the prediction of second order polynomial (SOP) models and were found to be 4.81, 0.88, 3.83 and 1.59 for rehydration ratio, scavenging activity, nonenzymatic browning and hardness (<10) indicated the deviation between experimental and predicted values are low.[69] The mean relative

deviation ($(R_d)_{RSM}$) between experimental and predicted values for the four responses was found to be 11.84%. On the contrary, results of dried peel presented in Table 6.9 revealed that rehydration ratio, scavenging activity and nonenzymatic browning had R^2 values of 0.88, 0.84 and 0.86 respectively which are also in agreement with the value of adj-R^2 and predicted R^2. Similarly, the adequate precision for the models were found Y_{RR} = 12.19, Y_{SA},= 14.68 and Y_{NEB} = 9.42. The CV% were recorded Y_{RR} = 8.38, Y_{SA}= 5.67 and Y_{NEB} = 7.93 (<10) confirmed less deviation between experimental and predicted values. ($(R_d)_{RSM}$) between experimental and predicted values for all the three responses was 9.67%.

Table 6.8 ANOVA for experimental results of general factorial design of dried pulp

Source	DF	RR			SA (%)			NEB (%)			Hardness (N)		
		CE	SE	*p*-value	CE	SE	*p*-value	CE	SE	*p*-value	CE	SE	*p*-value
Model	10	2.34	0.01	<0.0001	40.37	0.04	<0.0001	21.00	0.09	<0.0001	52.10	0.09	<0.0001
x_1	1	0.14	0.02	<0.0001	0.018	0.08	0.9901	-0.37	0.18	0.0008	1.35	0.19	<0.0001
x_2	1	0.05	0.25	<0.0001	$7.27x10^{-3}$	0.08	<0.0001	-0.19	0.18	<0.0001	$2.19x10^{-3}$	0.19	<0.0001
x_3	1	-0.01	0.25	<0.0001	$-2.70x10^{-3}$	0.08	<0.0001	$2.89x10^{-3}$	0.18	<0.0001	-0.69	0.19	<0.0001
$x_1 x_2$	1	-0.07	0.26	<0.0001	1.03	0.69	<0.0001	-0.39	0.18	<0.0001	-0.60	0.19	<0.0001
$x_1 x_3$	1	-0.24	0.25	<0.0001	-0.30	0.69	<0.0001	-0.40	0.16	<0.0001	4.30	0.16	<0.0001
$x_2 x_3$	1	-0.21	0.22	<0.0001	-0.36	0.69	<0.0001	$-3.70 x10^{-3}$	0.16	<0.0001	2.92	0.16	<0.0001
x_1^2	1	-0.08	0.22	<0.0001	0.24	0.69	<0.0001	2.73	0.16	<0.0001	-0.11	0.16	<0.0001
x_2^2	1	0.03	0.22	<0.0001	0.13	0.69	<0.0001	-0.40	0.16	<0.0001	1.19	0.16	<0.0001
x_3^2	1	0.04	0.22	<0.0001	-0.09	0.69	<0.0001	-1.09	0.16	<0.0001	0.92	0.16	<0.0001
Std. Dev		0.11			0.36			0.80			0.83		
R^2		0.90			0.78			0.83			0.97		
Adj. R^2		0.89			0.75			0.81			0.96		
Pred. R^2		0.87			0.70			0.78			0.96		
Adeq. precision		27.57			14.68			19.76			54.77		
C.V %		4.81			0.88			3.83			1.59		
PRESS		1.17			11.80			60.09			63.51		

DF = degree of freedom; CE = coefficient estimate; SE = standard error; C.V = coefficient of variance; PRESS = predicted error sum of square; RR = rehydration ratio; SA = scavenging activity; NEB = non enzymatic browning; H= hardness

Table 6.9 ANOVA for experimental results of general factorial design of dried peel

Source	DF	RR			SA (%)			NEB (%)		
		CE	SE	*p*-value	CE	SE	*p*-value	CE	SE	*p*-value
Model	10	6.68	0.12	<0.0001	81.28	0.04	<0.0001	31.34	1.06	<0.0001
x_1	1	0.76	0.89	<0.0001	-4.29	0.52	0.9901	0.92	1.49	0.0008
x_2	1	-0.24	0.29	<0.0001	-0.05	0.68	<0.0001	0.43	0.08	<0.0001
x_3	1	0.18	0.23	<0.0001	0.24	0.75	<0.0001	-4.28	0.45	<0.0001
$x_1 x_2$	1	2.50×10^{-3}	0.34	<0.0001	-0.29	0.36	<0.0001	-0.55	0.46	<0.0001
$x_1 x_3$	1	-0.17	0.25	<0.0001	0.31	1.66	<0.0001	0.90	0.60	<0.0001
$x_2 x_3$	1	0.065	0.43	<0.0001	0.21	1.19	<0.0001	-1.30	0.28	<0.0001
x_1^2	1	0.17	0.33	<0.0001	0.53	1.46	<0.0001	1.03	0.65	<0.0001
x_2^2	1	0.15	0.41	<0.0001	-0.49	0.23	<0.0001	0.86	0.03	<0.0001
x_3^2	1	-0.22	0.26	<0.0001	-0.61	0.61	<0.0001	2.18	0.85	<0.0001
Std. Dev		0.36			1.99			1.95		
R^2		0.88			0.84			0.86		
Adj. R^2		0.81			0.78			0.75		
Pred. R^2		0.77			0.71			0.72		
Adeq. precision		12.19			14.68			9.42		
C.V %		8.38			9.67			7.93		
PRESS		11.38			56.19			60.22		

DF = degree of freedom; CE = coefficient estimate; SE = standard error; C.V = coefficient of variance; PRESS = predicted error sum of square; RR = rehydration ratio; SA = scavenging activity; NEB = non enzymatic browning

6.7.2 Modeling of the process parameters by artificial neural network

Based on the experimental works an ANN was developed by using feed forward ANN architecture viz., multilayer perceptron (MLP) with sigmoid function. The experimental design and the data obtained from experiments were used for training the network. The MLP network used in the present study consists of 3 input, 5 hidden layers and 4 output nodes (Fig. 6.10). Temperature (X_1), slice thickness (X_2) and pretreatment (X_3) are the three inputs and rehydration ratio (Y_{RR}), scavenging activity (Y_{SA}), nonenzymatic browning (Y_{NEB}) and hardness (Y_H) are the four output nodes. The aim of ANN modeling was to optimize the neural network with minimum errors in training and testing.

The values of 'u', 'w', 'Th' and 'To' were obtained through random number generation. For all the data, single computational data set was used and the final values of all the matrices were obtained after the 2000 computational cycles. The final values of matrices 'u', 'w', 'Th' and 'To' were obtained by the above process are given below.

a) For pulp slices

$$u = \begin{bmatrix} -0.01 & 0.12 & 1.19 & -0.23 & -0.07 \\ -1.51 & -0.16 & -0.18 & 0.64 & 3.46 \\ -0.15 & 1.16 & -0.12 & -2.22 & 0.96 \end{bmatrix}$$

$$w = \begin{bmatrix} 0.07 & 2.51 & -1.61 & 3.73 \\ 2.66 & 3.28 & -1.54 & -0.12 \\ 3.66 & -4.02 & 2.48 & -1.29 \\ -0.92 & 0.61 & 3.28 & 0.97 \\ -1.65 & 0.41 & -0.66 & -3.30 \end{bmatrix}$$

$$Th = \begin{bmatrix} 0.29 \\ -1.25 \\ 0.48 \\ -2.20 \\ 4.18 \end{bmatrix} \qquad To = \begin{bmatrix} -1.29 \\ -0.81 \\ -0.62 \\ 0.93 \end{bmatrix}$$

b) For peel

$$u = \begin{bmatrix} -0.38 & 0.78 & 1.10 & -0.03 & -0.44 \\ -1.37 & -0.36 & -0.19 & 0.74 & 1.67 \\ -0.31 & 0.69 & -1.87 & -1.55 & 0.12 \end{bmatrix}$$

$$w = \begin{bmatrix} 0.24 & 1.41 & -1.69 & 2.27 \\ 1.35 & 2.27 & -1.48 & -0.80 \\ 2.97 & -2.71 & 2.42 & -2.61 \\ -1.09 & 0.97 & 4.85 & 1.01 \\ -2.96 & 0.28 & -1.21 & -2.23 \end{bmatrix}$$

$$Th = \begin{bmatrix} 1.69 \\ -1.48 \\ 0.58 \\ -1.19 \\ 1.94 \end{bmatrix} \qquad To = \begin{bmatrix} -2.67 \\ -0.66 \\ -1.13 \\ 1.55 \end{bmatrix}$$

The final values of 'u', 'w', 'Th' and 'To' are applied in Eq. (6.11 – 6.14) to obtain the coded values of 'yo' which was converted to real values to obtain the corresponding predicted response.

6.7.3 Comparative study between RSM and ANN model

The relative deviation ($(R_d)_{ANN}$) between experimental and predicted values of dried pulp for rehydration ratio (Y_{RR}), scavenging activity (Y_{SA}), nonenzymatic browning (Y_{NEB}) and hardness (Y_H) by ANN model was found to be 2.40, 1.13, 1.30 and 0.72 respectively having a mean deviation of 1.39%. On the other hand the values of ($(R_d)_{RSM}$) between experimental and predicted values for Y_{RR}, Y_{SA}, Y_{NEB} and Y_H are 6.97, 6.14, 4.31and 11.02% respectively with mean relative deviation of 7.11%. Similarly, for dried peel $(R_d)_{ANN}$ for Y_{RR}, Y_{SA} and Y_{NEB} were 1.35, 0.85, 2.61 respectively with mean deviation of 1.60% and ($(R_d)_{RSM}$ between experimental and predicted values were 6.45, 6.67, 6.55% with mean deviation of 6.55%. From the values of both pulp and peel it is observed that the mean relative deviation obtained by ANN method is ($(R_d)_{ANN}$) absolutely smaller than ($(R_d)_{RSM}$) obtained by RSM. This comparison shows the

responses can be more effectively predicted by ANN method with less error than RSM. Figs. 6.12a-d and 6.13a-c illustrate the plots of the experimental and predicted values for all the four responses in case of pulp and three responses in case of peel respectively. The plot revealed that predicted values are very close to the experimental values. The result showed that RSM models are larger than ANN models, indicating that the latter has higher modeling ability over RSM model for drying of culinary banana. Similar result of better predictions obtained with ANN over RSM has also been reported by Miletic et al.[70]

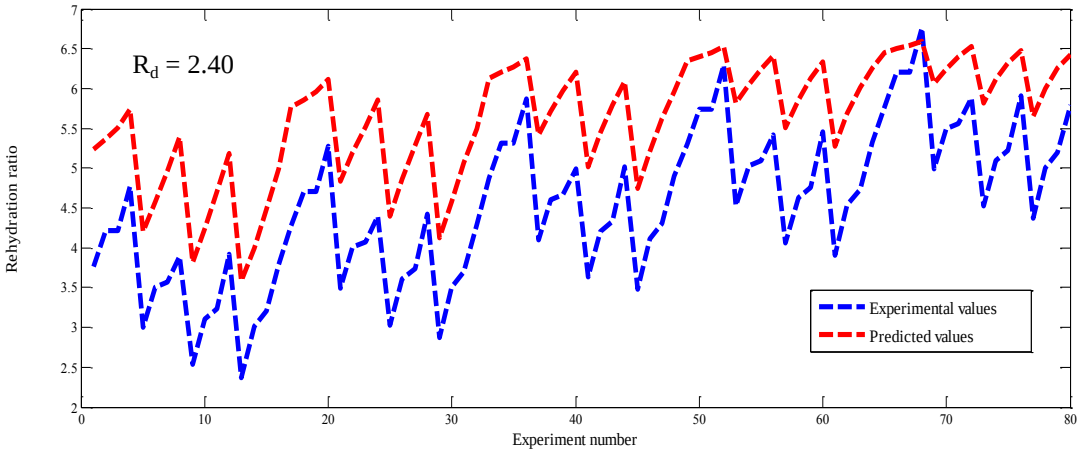

Fig. 6.12a Correlation between experimental and predicted values for rehydration ratio of dried pulp slices

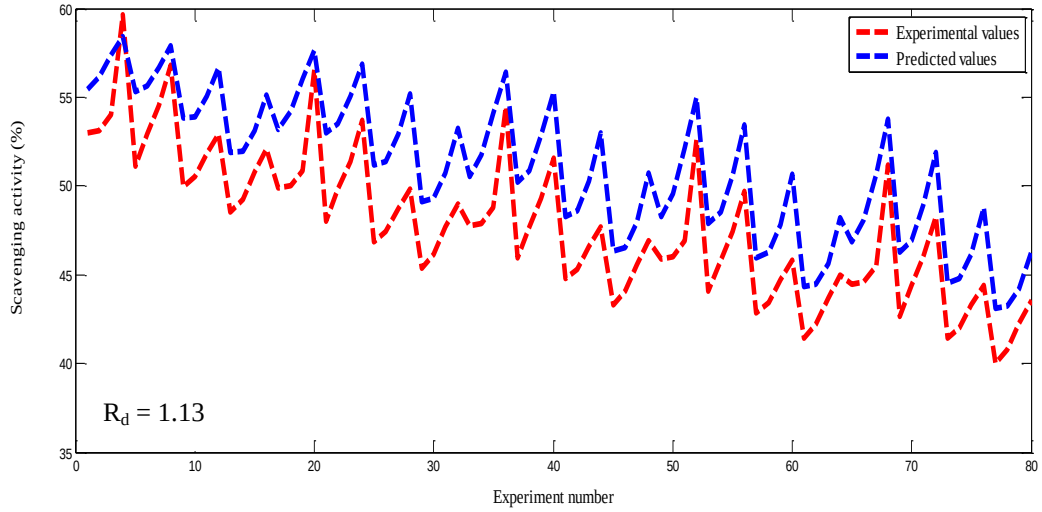

Fig. 6.12b Correlation between experimental and predicted values for scavenging activity dried pulp slices

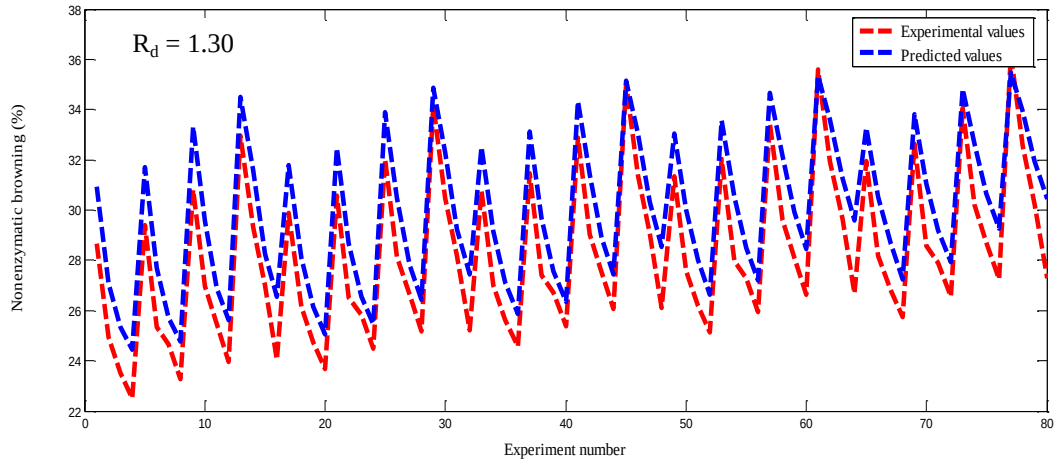

Fig. 6.12c Correlation between experimental and predicted values for nonenzymatic browning of dried pulp slices

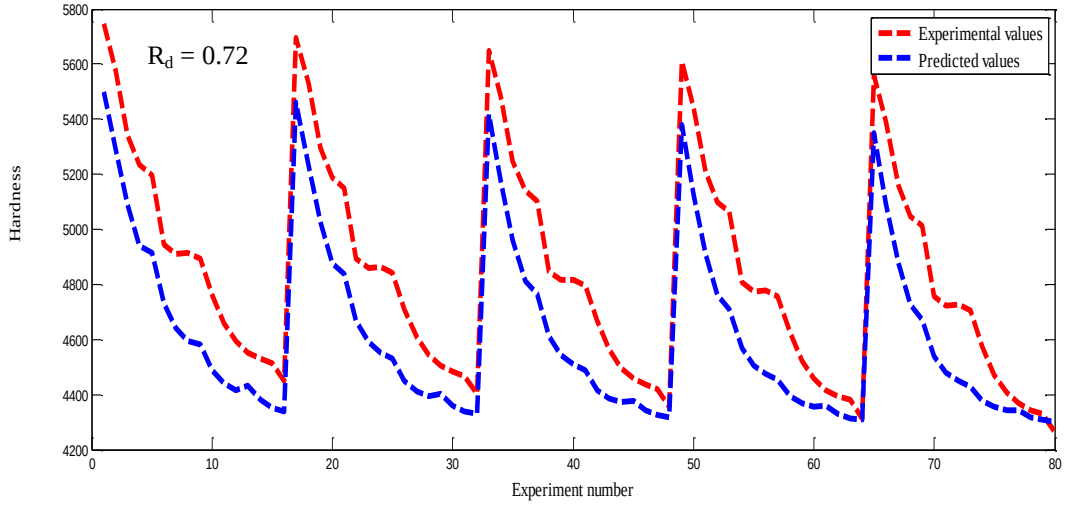

Fig. 6.12d Correlation between experimental and predicted values for hardness of dried pulp slices

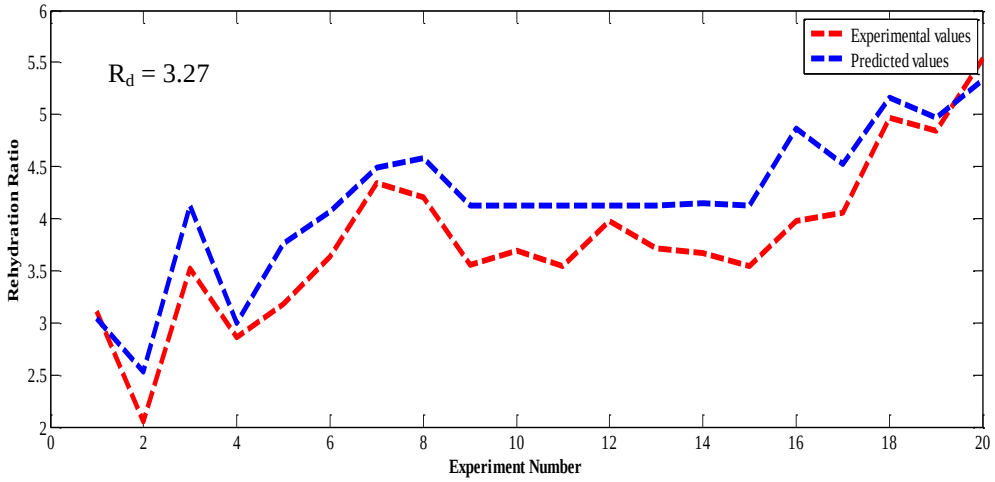

Fig. 6.13a Correlation between experimental and predicted values for rehydration ratio of dried peel

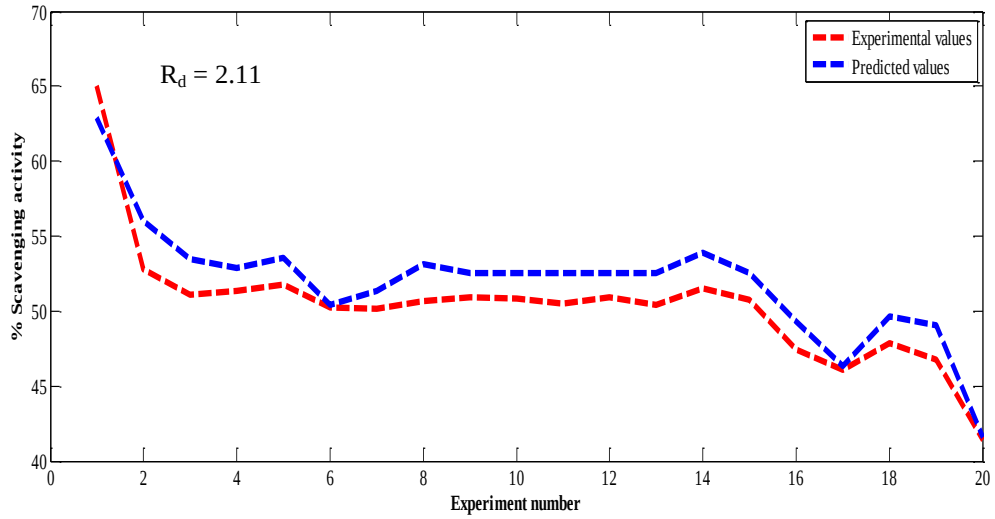

Fig. 6.13b Correlation between experimental and predicted values for scavenging activity dried peel

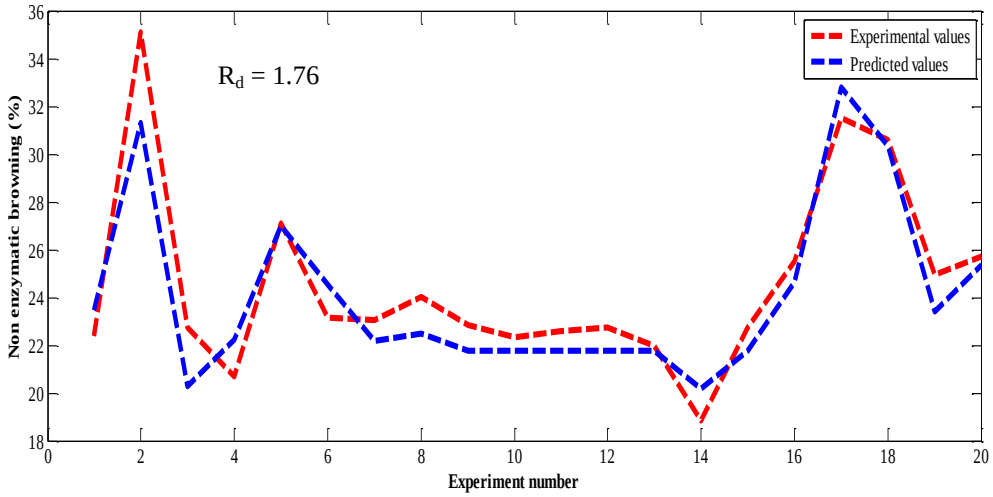

Fig. 6.13c Correlation between experimental and predicted values for nonenzymatic browning of dried peel

6.7.4 Effect of independent variables on rehydration ratio of dried culinary banana

The experimental result shows that a maximum rehydration ratio of 6.20 was obtained for 6 mm thickness samples dried at 76^{o}C in case of pulp, and for peel sample maximum rehydration ratio of 7.65 was recorded in 4 mm thick paste dried at 71^{o}C. The relative influence of temperature (X_1), thickness (X_2) and pretreatment (X_3) on rehydration ratio is presented as $(\Delta y_{RR})x_1$, $(\Delta y_{RR})x_2$, $(\Delta y_{RR})x_3$ respectively and the corresponding values are presented in Tables 6.10 and 6.11 for pulp and peel respectively . The magnitude of $(\Delta y_{RR})x_1$, $(\Delta y_{RR})x_2$, $(\Delta y_{RR})x_3$ shows that temperature has highest effect on rehydration ratio followed by pretreatment and thickness. The sign of the computed output values of output layer neurons (Δy_{RR}) are positive for temperature and pretreatment but negative for slice thickness. Hence temperature and pretreatment have positive effects on rehydration ratio of the final products. With the increase in temperature the rehydration ratio also increased and less damage occurred to the pore structure. On the contrary prolonged heating at lower temperature caused greater shrinkage and decreased the rehydration ratio. The obtained results are in line with vacuum drying of onion slices.[22] The relative effect of pretreatment on rehydration ratio ($(\Delta y_{RR})x_2$) revealed that pretreatment could enhance the effect on rehydration. Doymaz[71] studied rehydration characteristics of white button

mushroom and obtained similar effect of pretreatment on rehydration in the mushroom slices which also supports our results. Slice thickness had negative effect on rehydration ratio indicating that with an increase of thickness, the rehydration ratio decreased. The negative effect of slice thickness on rehydration ratio has also been reported by Abano and Sam-Amoah[30] in case of ripe banana slices.

6.7.5 Effect of independent variables on DPPH radical scavenging activity

The radical scavenging activity of vacuum dried culinary banana was in the range of 39.99-59.67% in pulp and 80.56-88.78% in case of dried peel. The computed output value $(\Delta y_{SA})x_1 = -0.42$ for pulp (Table 6.10) and $(\Delta y_{SA})x_1 = -0.98$ for peel (Table 6.11) of output layer neurons which conclude that the drying temperature has the highest negative impact on scavenging activity. Lower scavenging activity was observed when higher drying temperature was applied during the drying process. Erbay and Icier[72] also observed intense drying temperature decreased antioxidant activity and suggested that moderate temperature was desirable to increase the retention of antioxidant capacity of olive leaves during drying. The negative effect of temperature on scavenging activity has also been reported by Ozgur et al.[49] and found decreasing trend in antioxidant activity when leek leaves were dried at higher temperature. The production and accumulation of melanoid compounds from the Maillard reaction having an unstable degree of antioxidant activity can be responsible for the change in antioxidant activity at higher temperatures.[73]Slice thickness showed the negative effect on scavenging activity with magnitude of computed value of $(\Delta y_{SA})x_2 = -0.25$ and $(\Delta y_{SA})x_2 = -0.12$ while pretreatment showed positive effect $(\Delta y_{SA})x_3 = 0.25$ and $(\Delta y_{SA})x_3 = 0.67$ for pulp and peel respectively. The samples pretreated with citric acid revealed that the retention of scavenging power was higher for those samples treated with higher concentration of citric acid. Abou-Arab et al.[74] have reported that roselle plant samples treated with 1% citric acid exhibited higher value of total antioxidant activity compared to untreated sample extract which corroborates our results.

6.7.6 Effect of independent variables on colour of dried culinary banana

The result revealed that nonenzymatic browning occurred at a faster rate when dried at higher temperature compared to lower temperature. The maximum value of optical index was 22.50% and 41.34% at 80^{o}C in both pulp and peel. The results of Δy_{NEB} (relative influence of independent variables on nonenzymatic browning) revealed that pretreatment has highest effect followed by drying temperature and slice thickness (Tables 6.10 and 6.11). The value of relative influence of temperature $(\Delta y_{NEB})x_1$=0.23 (pulp) and $(\Delta y_{NEB})x_1$ = 0.27 (peel) and slice thickness $(\Delta y_{NEB})x_2$ = 0.24 (pulp) and $(\Delta y_{NEB})x_2$ = 0.36 on nonenzymatic browning indicates positive effect. Increase in temperature and slice thickness caused increase in nonenzymatic browning which was unlike with pretreatment i.e. it showed negative $(\Delta y_{NEB})x_3$ = -0.51 and $(\Delta y_{NEB})x_3$ = -0.67 effects in both pulp and peel respectively. Within the experimental range it was obtained that increase in concentration of citric acid resulted in decrease of nonenzymatic browning value. Hence the colour value can be minimized by adopting higher concentration of pretreatment coupled with lower drying temperature. Similar effects on nonenzymatic browning have been observed in drying of onion and strawberry.[47] Thuwapanichayanan et al.[22] also reported drying of dessert banana at lower temperatures to preserve its colour.

6.7.7 Effect of independent variables on hardness of dried culinary banana slices

The hardness of dried culinary banana slices is affected by drying temperatures and is associated with composition and structure of cell walls. The samples dried at 40^{o}C required lowest maximum force (42.63N) to obtain the force deformation curve whereas samples dried at 80^{o}C required highest maximum force (57.45 N). Thickness [$(\Delta y_H)x_2$ = -0.63] has highest impact on hardness (Table 2) followed by pretreatment [$(\Delta y_H)x_3$ = -0.18] and temperature [$(\Delta y_H)x_1$ = -0.15]. The relative influence of the independent variables on texture shows that all the parameters have negative effect on hardness of dried culinary banana slices. The results revealed that texture of dried culinary banana slices in terms of hardness was found minimum in samples dried at higher temperature. The resultant product is having more rehydration rate and may be attributed to the surface hardening of samples dried at lower temperature for longer time. Surface hardening reduces the rate of drying and produces banana slice having dry surface and a moist

interior which on rehydration absorbs water more slowly and does not regain the firm texture associated with the fresh material. It can be minimized by drying the product at a higher temperature to prevent excessively high moisture gradients between the interior and the surface of the food. On the other hand samples dried at higher temperature (80^{o}C) possess large porous structure which required lowest maximum force and in addition, drying at higher temperature leads more volume and a crust on the surface of the product giving better reconstitution properties. A excellent texture of banana slices obtained at higher temperature has also been reported by Raikham et al.[75]

Table 6.10 Relative influence of the coded values of independent variables on the responses Y_{RR}, Y_{SA}, Y_{NEB}, Y_H of pulp

X_1	X_2	X_3	Δy_{RR}	(R_d)	Δy_{SA}	(R_d)	Δy_{NEB}	(R_d)	Δy_H	(R_d)
+1	0	0	$(\Delta y_{RR})x_1 = 0.46$		$(\Delta y_{SA})x_1 = -0.42$		$(\Delta y_{NEB})x_1 = 0.23$		$(\Delta y_H)x_1 = -0.15$	
-1	0	0								
0	+1	0	$(\Delta y_{RR})x_2 = -0.28$	2.40	$(\Delta y_{SA})x_2 = -0.25$	1.13	$(\Delta y_{NEB})x_2 = 0.24$	1.30	$(\Delta y_H)x_2 = -0.63$	0.72
0	-1	0								
0	0	+1	$(\Delta y_{RR})x_3 = 0.29$		$(\Delta y_{SA})x_3 = 0.25$		$(\Delta y_{NEB})x_3 = -0.51$		$(\Delta y_H)x_3 = -0.18$	
0	0	-1								

Δy_{RR} = computed output values of output layer neurons for rehydration ratio; Δy_{SA}= computed output values of output layer neurons for scavenging activity; Δy_{NEB} = computed output values of output layer neurons for non-enzymatic browning; Δy_H = computed output values of output layer neurons for hardness; R_d = relative deviation

Table 6.11 Relative influence of the coded values of independent variables on the responses Y_{RR}, Y_{SA}, Y_{NEB} of peel

X_1	X_2	X_3	Δy_{RR}	(R_d)	Δy_{SA}	(R_d)	Δy_{NEB}	(R_d)
+1	0	0	$(\Delta y_{RR})x_1 = 0.65$		$(\Delta y_{SA})x_1 = -0.98$		$(\Delta y_{NEB})x_1 = 0.27$	
-1	0	0						
0	+1	0	$(\Delta y_{RR})x_2 = -0.76$	3.27	$(\Delta y_{SA})x_2 = -0.12$	2.11	$(\Delta y_{NEB})x_2 = 0.36$	1.76
0	-1	0						
0	0	+1	$(\Delta y_{RR})x_3 = 0.54$		$(\Delta y_{SA})x_3 = 0.67$		$(\Delta y_{NEB})x_3 = -0.67$	
0	0	-1						

Δy_{RR} = computed output values of output layer neurons for rehydration ratio; Δy_{SA}= computed output values of output layer neurons for scavenging activity; Δy_{NEB} = computed output values of output layer neurons for non-enzymatic browning; R_d = relative deviation

Table 6.12 Results of optimized values by genetic algorithm

Sample	Temp (X_1)	Thickness (X_2)	Treatment (X_3)	Y_{RR}	Y_{SA}	Y_{NEB}	Y_H
Pulp	76 ^oC	6 mm	1%	6.20	48.63%	25.00%	43.63N
Peel	71	4 mm	1%	7.65	76.76	33.76	-

6.7.8 Microstructure evaluation by scanning electron microscope

Scanning electron micrographs (SEM) of culinary banana samples dried at various temperatures are illustrated in Fig. 6.14 (pulp) and Fig. 6.15 (peel) which can be correlated to the texture (hardness) of the final product. The effect of drying temperature (40-80^{o}C) on the microstructure of culinary banana was characterised by small or large pores. From the figures it was found that the samples dried at 40^{o}C created large numbers of smaller size pores and led to the dense structure of the final dried product. The pore formation in dried sample is due to the evaporation of water vapour from the cells which led to the development of internal pressure and breakage of the sample tissues, resulting in the formation of pores. Abbasi et al.[41] also reported that low temperature coupled with long time heating causes stress in the cellular structure of food which leads to the denser structure with large number of smaller size pores which supports the present results. The number of pore size increased with increase in drying temperature as illustrated in figures. Results revealed that when samples were dried at 80^{o}C, highly porous final product was obtained with larger pore size. It can be concluded that drying at higher temperature may raise the hydrostatic pressure gradient of moisture between inside and outside of the dried samples which subsequently leads to the large pores and voids.[42] These pores and voids space not only affect the textural property, but also the transport phenomenon such as diffusivities of gases and liquids in the sample and resulting higher rate of effective moisture diffusivity at higher drying temperature[31] which corroborates our findings. Several other workers also reported similar results in different fruits.[22, 44, 45]

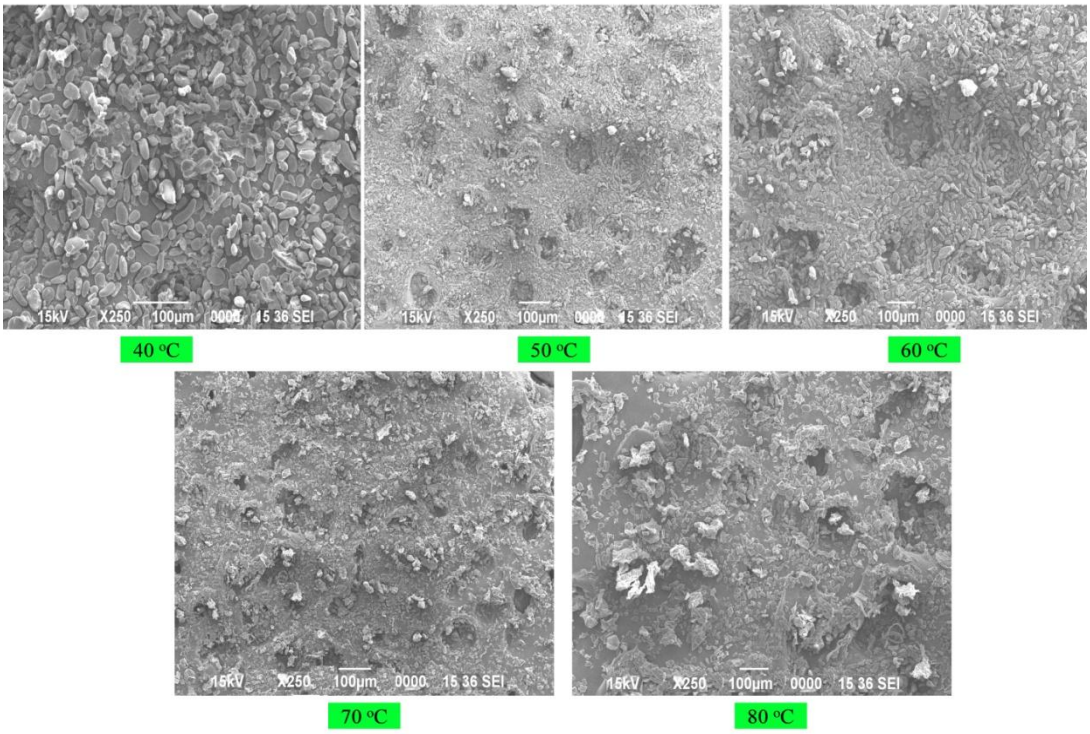

Fig. 6.14 Scanning electron micrographs pulp dried at various temperatures

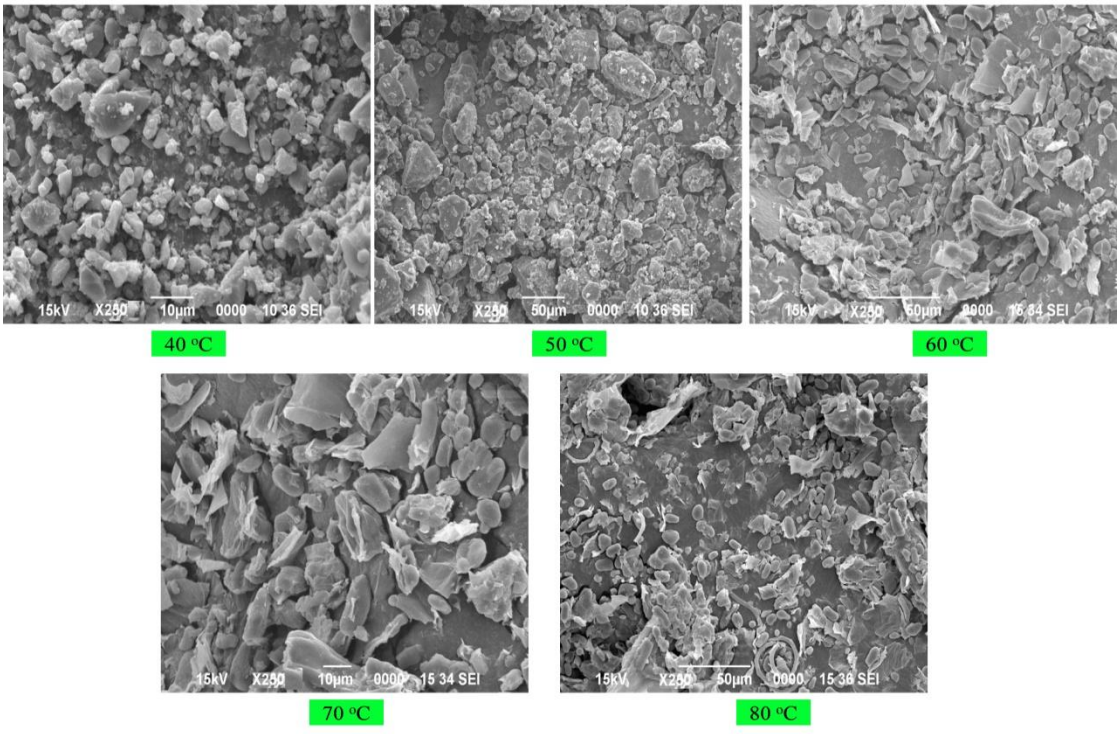

Fig. 6.15 Scanning electron micrographs of peel dried at various temperatures

6.7.9 Optimization of process parameters by GA

The prognostic models of responses viz., rehydration ratio (Y_{RR}), scavenging activity (Y_{SA}), nonenzymatic browning (Y_{NEB}) and hardness (Y_H) of dried samples were further used for attaining the optimum process conditions for drying culinary banana under vacuum drying condition. For the optimization process the fitness function has been formulated for maximization of rehydration ratio and scavenging activity and minimization of nonenzymatic browning and hardness. The modeled parameter values obtained from ANN were optimized using GA and hence the output parameters of ANN model ('u', 'w', 'Th' and 'To') was considered as input for GA optimization process. Precision for determining the string lengths of GA series was obtained based on the maximum and minimum values of independent variables. The optimal condition was selected from a pool of ANN/GA responses on the basis of highest fitness value. The optimum process conditions (Table 6.12) obtained from hybrid ANN/GA for dried culinary banana pulp was drying temperature (X_1=76^{o}C), slice thickness (X_2 = 6 mm) and pretreatment concentration (X_3 = 1% of citric acid). The above condition resulted in rehydration ratio of 6.30, scavenging activity up to 48.63%, nonenzymatic browning of 25% and hardness value 43.63N. Similarly, the optimum process conditions obtained for drying of peel was drying temperature (X_1=71^{o}C), slice thickness (X_2 = 4 mm) and pretreatment concentration (X_3 = 1% of citric acid) to obtained final product having rehydration ratio of 7.65, scavenging activity up to 76.76% and nonenzymatic browning of 37.75%. At optimized combination the experiment was conducted in triplicate and average of the obtained responses was presented.

6.7.10 Validation of the GA

Predicted optimal conditions using ANN/GA were applied to obtain the maximum rehydration ratio and scavenging activity and minimum nonenzymatic browning and hardness. The relative deviation (R_d) between experimental and predicted values presented in Table 6.13 for dried pulp was 1.13, 2.27. 2.94 and 1.28 for rehydration ratio, scavenging activity, nonenzymatic browning and hardness respectively. On the other hand, the R_d between experimental and predicted values for peel (Table 6.14) was 1.18, 3.56 and 2.74 for rehydration ratio, scavenging activity and nonenzymatic browning respectively.

Table 6.13 Relative deviation between experimental and predicted values of dried pulp

	Y_{RR}	Y_{SA}	Y_{NEB}	Y_H
Experimental Values	6.20	47.09	23.98	44.43
Predicted value from hybrid ANN and GA	6.30	48.63	25.00	43.63 N
Relative deviation (R_d)	1.13	2.27	2.94	1.28

Table 6.14 Relative deviation between experimental and predicted values of dried peel

	Y_{RR}	Y_{SA}	Y_{NEB}
Experimental Values	7.65	76.76	37.75
Predicted value from hybrid ANN and GA	7.77	78.84	34.58
Relative deviation (R_d)	1.18	3.56	2.74

6.8 Conclusions

ANN predicted the quality attributes of vacuum dried culinary banana undergoing at various drying temperatures. Comparison of the performance of ANN and RSM with their modeling, prediction and optimization using the experimental data for vacuum dehydration process of culinary banana revealed ANN models are found to be capable of better predictions for responses (rehydration ratio, scavenging activity, nonenzymatic browning and hardness) compared to RSM. Maximization of responses of rehydration ratio and scavenging activity percentage and minimization of nonenzymatic browning and hardness were obtained through ANN modeling followed by GA optimization process. Therefore, ANN proved to be a useful tool for correlation and simulation of vacuum drying parameters of culinary banana. The results demonstrated that drying temperature, sample thickness, and pretreatment had significant effects on rehydration ratio of dried slices. Both drying temperature and pretreatment had positive effect on rehydration ratio and the effect of drying temperature was most significant. Better quality product with higher scavenging activity was obtained when banana slices of lesser thickness were dried at low temperatures. Increased temperature and thickness enhanced enzymatic

browning but pretreatment reduced the browning and retained the colour of the product. Taking into account drying time and quality of the final product, it was proposed that a drying temperature at 76^{o}C with citric acid pre treatment of 1% concentration and a sample thickness of 6 mm should be used for vacuum drying of culinary banana slices. In addition, it was also suggested that drying temperature of 71^{o}C, with 1% citric acid pretreatment and paste thickness of 4 mm could be used for vacuum drying of peel. The thin layer vacuum drying is suitable for drying both culinary banana pulp slices and peel paste, and the process exhibited marked decrease in drying time and retained maximum rehydration ratio, scavenging activity and minimum nonenzymatic browning and hardness under the optimised drying conditions.

C) Moisture sorption isotherm of culinary banana flour and its antioxidant stability during storage

6.9 Introduction

The culinary banana, a nutritionally rich crop of local importance has not gain much attention in terms of value addition and fall under the category of underutilized crop. The world depends for its basic diet of carbohydrates, fats and proteins on a very limited number of crop species and mainly wheat, rice and maize dominate human consumption of carbohydrate.[76] For improvement in food security it is needed to include modification of these and other staple crops. In the diversification of food security, culinary banana could play an essential role as it is very rich in the chemical compositions.

One of our concerns is to utilize this culinary banana for the benefit of society in terms of nutrients, functionality and healthy diet. The culinary banana can be utilized in various forms as a raw material in variety of domestic and regional products.[77] The value added products like crisps, fritter, wine, beer, domestic and artisanal flour, starch, vinegar and chunk or purees to be used as ingredients in culinary preparations could be prepared. Unfortunately, very few value added products are available so far. As mentioned, culinary banana flour though nutritionally rich but is susceptible to deteriorative reactions like lipid oxidation and microbial spoilage during long term storage. Therefore, proper designing of packaging and storage system are merely important for such food types.

To serve the purpose, MSI study is considered as one of the most potent tools for determining suitable packaging and storage conditions and to optimize product quality retention and biological stability.[78] The relationship between total moisture content and the water activity of the food at a constant temperature gives MSI. Adsorption and desorption isotherms are termed when the material reaches equilibrium by wetting or drying, respectively.[79] An adsorption isotherm is achieved by keeping a dry material in an increasing relative humidity atmosphere and measuring the gain in weight due to water uptake. On the contrary, desorption isotherm is calculated by keeping an initially wet material under the same relative humidity conditions and loss in weight is measured.[80] MSI of most foods including the starchy ones follow nonlinear Langmuir adsorption model, which are generally type II isotherm and are sigmoidal in shape.[81]

For the prediction of food MSI, numerous empirical and semi-empirical mathematical models have been suggested in the literature.[82, 83] MSI studies on some starchy flours have also been studied by various researchers.[81, 84-87]

The objective of the present study is to evaluate the MSI of culinary banana flour which has been optimized at particular drying condition in our previous objective, and also to evaluate the applicability of various existing models for fitting the sorption data. Additionally, the chemical stability of flour in terms of its antioxidant has also been examined through 120 days storage at 25^{o}C. It is expected that this study would be useful to the low moisture food industry where culinary banana could promote its industrialization as high valued flour.

6.10 Materials and methods

6.10.1 Raw materials

Culinary bananas flour obtained at optimized drying conditions were taken for storage and MSI studies. All the chemicals and analytical salts required for present study was high purity AR grade supplied by Sigma-Aldrich (USA), HiMedia (India) and Merck (India).

6.10.2 Antioxidant stability during storage

The changes in antioxidant properties (radical scavenging activity and total polyphenols) were evaluated during storage. The Petri dishes filled with flour samples were placed in hermetically sealed glass desiccators containing supersaturated solution of NaCl (75% RH) and stored at 25^{o}C and analysis viz. DPPH radical scavenging activity and total polyphenols were analysed at every 15 days interval for 120 days.[88]

6.10.3 Moisture sorption isotherm (MSI) studies

To obtain the MSI of vacuum dried culinary banana flour equilibrium moisture content (EMC) method was followed. Eight saturated electrolyte solutions viz. lithium chloride (LiCl), magnesium chloride ($MgCl_2$), potassium carbonate (K_2CO_3), Magnesium nitrate ($Mg(NO_3)_2$),

potassium iodide (KI), sodium chloride (NaCl), potassium chloride (KCl), potassium sulphate (K_2SO_4) giving relative humidities (RH) varying between 11 to 97% were used.[88, 89] The RH of various salts at temperature ranged from 25-45^oC is presented in Table (6.15). Triplicate samples (3 g) were weighed in Petri dishes and kept inside hermetically sealed desiccators and maintained the particular RH with a different saturated salt solutions. The desiccators were placed inside an incubator chamber with air circulation (B.O.D. Incubator, Optics Technology, New Delhi, India) and specific temperature was maintained. The study was conducted at five temperatures (25, 30, 35 40 and 45^oC) which was selected based on our preliminary studies and literature.[90-92] In order to prevent microbial spoilage, 10 ml beaker containing toluene was also placed inside the desiccators having RH more than 75%.[93] The weight of each Petri dish containing samples were measured in every 3 days interval where the total time taken for removal, weighing and keeping samples back inside the desiccators was less than 20 s. This precaution helped minimization of atmospheric moisture during weighing.

On reaching equilibrium state (when difference in sample weight was less than 0.01 g between two successive readings) the final equilibrium moisture content (EMC) was calculated by measuring the difference in the weight loss before and after drying the samples at 105^oC for 3 h in a laboratory oven (Boi-Technics India) as described by Sant'Anna et al.[88] The total period of time taken by each samples to reach equilibrium was between 20-50 days depending on the RH conditions. In equilibrium, RH (which is now called as equilibrium relative humidity (ERH)) is related to water activity (a_w) as shown in Eq. (6.28) as described by Sahin and Summu[94]

$$a_w \equiv \frac{ERH}{100} \qquad \text{Eq. (6.28)}$$

Table 6.15 Equilibrium relative humidities of selected salt solutions at various temperature levels (Greenspan)[95]

Saturated salt solutions used	RH (%) at temperatures				
	25°C	30 °C	35 °C	40°C	45°C
LiCl	11.30	11.28	11.25	11.21	11.16
$MgCl_2$	32.78	32.44	32.05	31.60	31.10
K_2CO_3	43.16	43.17	43.17	43.17	43.17
$Mg(NO_3)_2$	52.89	51.40	49.91	48.42	46.93
KI	68.86	67.89	66.96	66.09	65.26
NaCl	75.29	75.09	74.87	74.68	74.52
KCl	84.34	83.62	82.95	82.32	81.74
K_2SO_4	97.30	97.00	96.71	96.41	96.12

6.10.4 Fitting to existing mathematical models and data analysis

To predict the adsorption monolayer moisture content at different temperatures, the experimental values of EMC and ERH were considered. Seven mathematical models (listed in Table 6.16) were fitted to experimental data (EMC versus a_w) and the constants of selected models were calculated by nonlinear regression using MATLAB (MathWorks, Inc., R2012b). In addition, biochemical stability during storage was conducted and values obtained (triplicate) were compared by ANOVA and Fisher's Least Significant Difference (LSD) with the help of OriginPro 8.5. These isotherm models are extensively used for food materials.[81, 88, 92] The goodness of fit and precision of selected models was on the basis of high coefficient of determination (R^2), low root mean square error (RMSE) and relative deviation percentage modulus (R_d) values. The R_d values lower than 10% is considered as an indication of a good fit for a practical purpose.[82] The value of R_d was evaluated using Eq. (6.29).

$$R_d = \frac{100}{N}\left[\sum_{i=1}^{N}\left(\frac{X_{pi}-X_{ei}}{X_{ei}}\right)\right] \quad \text{Eq. (6.29)}$$

Where, X_{ei} and X_{pi} are experimental and predicted EMC respectively and N is the total number of observations.

Table 6.16 Mathematical models used to fit the equilibrium moisture sorption isotherms of culinary banana flour

Model	Mathematical equation	Reference
Oswin	$M_w = A\left(\frac{a_w}{1-a_w}\right)^B$	Andrade et al.[96]
Smith	$M_w = A + Bln(1-a_w)$	Andrade et al.[96]
Curie	$M_w = exp(A + Ka_w)$	Curie [97]
Modified Halsey	$a_w = \exp\left(AM_w^{-C}\right)$	Basu et al.[98]
Lewicki-2	$M_w = A\left[\left(\frac{1}{a_w}\right)-1\right]^{B-1}$	Lewicki et al.[99]
Lewicki-3	$M_w = A\left[\left(\frac{1}{(1-a_w)^B}\right)-\left(\frac{1}{\{1+(a_w)^c\}}\right)\right]$	Lewicki et al.[100]
Peleg	$M_w = Aa_w^c + Ba_w^k$	Basu et al.[98]

M_w and M_o are equilibrium and monolayer moisture content respectively (g water. 100g dry matter^{-1}); a_w is the water activity (decimal); A, B, C and K are respective model constants

6.10.5 Determination of net isosteric heat of sorption

The net isosteric heat of sorption is used to estimate the energy requirements for drying processes and supply important information about the state of water in food products. They determine the extents of adsorbent temperature changes within the adsorber during the adsorption (exothermic) and desorption (endothermic) steps of the processes. The adsorbent temperature is a key variable in determining the local adsorption equilibria and kinetics on the adsorbent, which ultimately govern the separation performance of the processes.[101] As sorption data was obtained at different temperatures range, it is possible to determine the net isosteric heat of sorption at various moisture contents, calculated using the best-fit isotherm. The thermodynamic data on net isosteric heat of sorption is obtained from the study of sorption isotherm at two different temperatures using the integrated form of Clausius-Clapeyron equation given below.[89]

$$ln\left(\frac{a_{w1}}{a_{w2}}\right) = \left(\frac{q_{st}}{18R}\right)\left[\frac{1}{T_2} - \frac{1}{T_1}\right] \quad \text{Eq. (6.30)}$$

Where, $a_{w1}$and a_{w2} are water activities (decimal) at temperatures T_1 and T_2 respectively and q_{st} is net isosteric heat of sorption (kJ kg $^{-1}$water), R is the universal gas constant (8.314 kJ kmol^{-1}K^{-1}).

6.11 Results and discussion

6.11.1 Antioxidant stability during storage

The antioxidant stability of culinary banana flour during storage up to 120 days were evaluated and presented in Table 6.17. From the results it is revealed that the concentrations of both radical scavenging activity and polyphenols varied very little with respect to storage time. During initial storage days from 0 to 60 days, there was a very small significant difference and on increase in days of storage from 60 to 105 days, scavenging activity as well as polyphenols started to decrease significantly, but from 105 to 120 days no difference was observed. Culinary banana flour is a rich source of antioxidant and polyphenols and has potential to be used as functional ingredients in value added food products and its use in daily food may immensely benefit human health due to their antioxidant capabilities. There is several factors viz. light, temperature, air oxidation phenomenons which affect and degrade antioxidant and phenolic compounds.[102] Hence, the unnoticeable degradation observed in present study favourably concludes that storage of culinary banana flour at 25^{o}C up to 120 days does not affect its bioactive properties.

TABLE 6.17 DPPH radical scavenging activity and total polyphenols during storage

Storage time (days)	DPPH radical scavenging activity (% SA)	Total polyphenols (mg GAE*/100 g dry matter)
0	54.75±0.14^{e}	180.49±0.46^{e}
15	54.21±0.40^{de}	179.82±0.60^{d}
30	53.65±0.18^{d}	179.11±0.66^{de}
45	52.87±0.57^{de}	178.05±0.47^{cd}
60	51.64±0.37^{d}	177.37±0.60^{c}
75	50.02±0.65^{c}	176.56±0.81^{cd}
90	48.76±0.19^{b}	175.01±0.48^{b}
105	46.92±0.21^{a}	173.16±0.45^{a}
120	46.15±0.20^{a}	172.99±0.44^{a}

Values reported as mean±SD of three replications; mean followed by same small letter superscripts within a column are not significantly different (p>0.05); GAE* = Gallic acid equivalent

6.11.2 Moisture sorption characteristics of culinary banana flour

Studies of MSI of foods are important thermodynamic tools for predicting the interactions between water and food components and are of key interest as it provides practical information for drying, aeration and storage conditions.[103] The information on maximum stability during packaging and storage can also be predicted with the help of MSI study.[104] The sorption isotherms of culinary banana flour studied at five different temperatures viz. 25, 30, 35, 40, 45^{o}C are illustrated in Fig. 6.16 which was obtained for the EMC (dry basis) versus a_w. The isotherm obtained shown the sigmoid in shape resembling type II isotherm. As depicted in Fig. 6.16, in all the five temperatures, there was a gradual increase in EMC between 0.1 to 0.65 a_w which further showed sharp increase in EMC, beyond 0.65 a_w leading to type II isotherm of sigmoidal characteristics.[94, 105] The figure further illustrated that there was a decrease in EMC with increase in temperature but this effect was insignificant as revealed from ANOVA of experimental data at probability of p>0.05 and these results are in line with the findings of various authors in case of powder food materials. [84, 104, 106, 107] Type II isotherms have been reported to be good models for peel and unpeeled banana flour, tapioca, cassava and other

starchy flours.[84, 85, 108] The increasing behavior of adsorption isotherms beyond a_w level of 0.65 in all storage temperatures suggests that culinary banana flour would require an improved storage conditions with RH not exceeding 65%. As culinary banana flour is starchier therefore if RH exceeds 65%, increase in flour moisture content may occur. The crystalline regions of starch (amylopectin) are resistant to moisture diffusion, hence, flour moisture may affect the structure and can act as a plasticizer for amorphous region of amylose.[80, 81] On the contrary, if flour is stored at a_w lower than 0.3 the mobility of amylose region (amorphous) is limited which causes negligible plasticization effect.[81] In addition, it may also be concluded that at lower a_w level, the dielectric effect of water is not strong enough to break the interactive forces between individual sugar molecules. On increasing a_w the sugar molecules becomes more mobile and results in crystallization of amorphous molecules.[109]

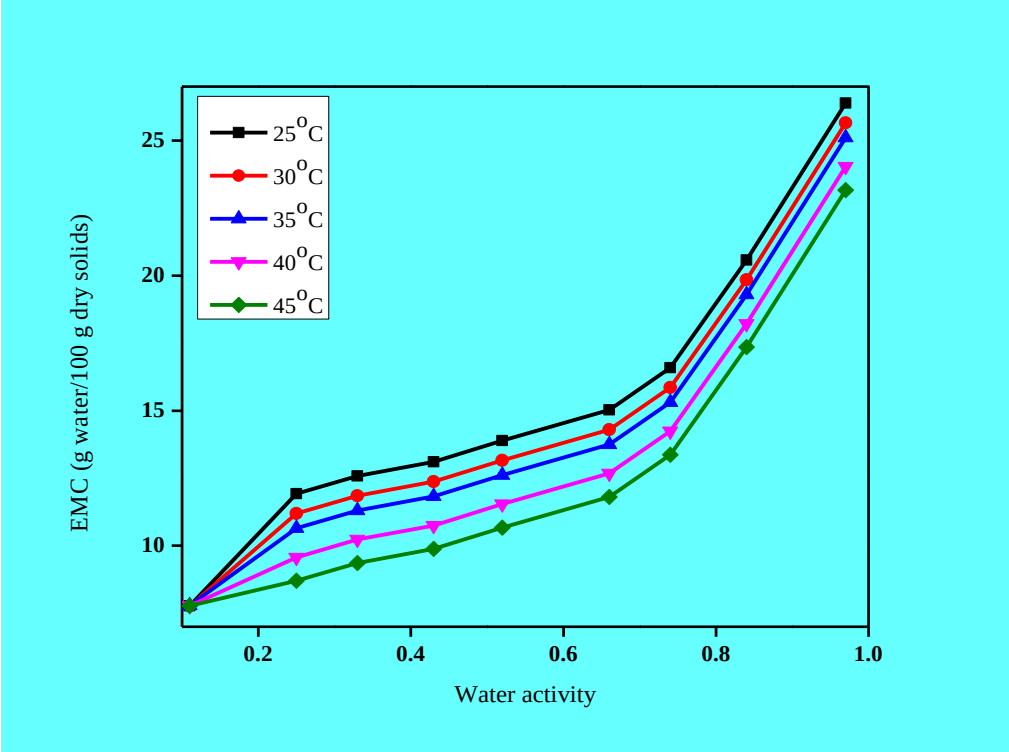

Fig. 6.16 Moisture sorption isotherm of culinary banana flour at different temperatures

6.11.3 Mathematical modeling and fitting of moisture sorption data

The EMC values obtained from experimental data at a_w range of 0.113 to 0.973 which was stored at five different temperatures (25-45^oC) were fitted to seven various sorption isotherm models and presented in Table 6.16. Mathematical models viz. Oswin, Smith, Curie, modified Halsey and Liwicki-2 with two parameters; Lewicki-3 with three parameters and Peleg with four parameters were fitted in those EMC data. The detail values of all respective constants as well as statistical parameters (R^2, adj. R^2, RSME and R_d) required to evaluate the best fitted model is presented in Table 6.18. It is revealed that in all the storage conditions, Peleg model having four parameters showed the highest coefficient of determination (R^2) with lower values of relative deviations (R_d) which was below 10% in all the five storage temperatures (Table 6.18). At 25^oC, the Peleg model values of R^2 and R_d were 0.998 and 6.83% respectively, which at 30^oC it was, R^2=0.995 and R_d = 4.22%. Similarly at 35^oC, it was, R^2=0.989 and R_d = 6.33%, at 40^oC it was, R^2=0.996 and R_d = 5.43% and finally at 45^oC, it recorded R^2=0.997 and R_d = 3.44%. These results describe that Peleg model stands first among all the models used in fulfilling the necessary criteria desired for the model to be the best fitted (Figs. 6.17a-6.17e). Hence, it can be concluded that Peleg model is more precise to describe and predict the EMC of culinary banana flour in the temperature range studied. Peleg model indicated the acceptability of this model as the most suitable model in order to use in the MSI study of culinary banana flour. According to the review of Andrade et al.[96] Peleg model always presents same or even better suitability than GAB model, which supports our findings. Several researchers have also found the Peleg model to be the most suitable model in prediction of EMC of various starchy powders such as Yam,[110] potato[111] and pistachio nut[112] at different storage temperatures. Lewicki-2 model with two parameters was the second best model found with better fitting to predict the EMC of culinary banana flour. In all the five storage temperatures the R^2 and R_d values were in the range of 0.979-0.986 and 7.46-10.45%. It is prudent to conclude Peleg and Lewicki-2 are more acceptable and suitable models to predict the EMC of culinary banana flour in the temperature range studied and was in the order of Peleg>Lewicki-2.

Table 6.18 Sorption isotherm models and their respective constants and statistical parameters

Storage temperature 25°C								
Model	**A**	**B**	**C**	**K**	**R^2**	**Adj. R^2**	**RMSE**	**R_d (%)**
Oswin	13.80	0.192	-	-	0.973	0.969	0.947	9.36
Curie	2.496	-	-	7.712	0.931	0.921	1.521	9.99
Smith	23.510	-7.712	-	-	0.880	0.863	2.005	10.83
Modified Halsey	9.844	-	0.583	-	0.831	0.806	2.382	11.48
Lewicki-2	**13.80**	**0.808**	**-**	**-**	**0.979**	**0.969**	**0.846**	**8.95**
Lewicki-3	10.861	0.296	-24.180	-	0.926	0.902	1.698	10.87
Peleg	**16.94 3**	**11.95 1**	**6.608**	**0.308**	**0.988**	**0.980**	**0.764**	**6.83**
Storage temperature 30°C								
Oswin	13.16	0.197	-	-	0.978	0.975	0.828	9.24
Curie	0.812	-3.127	-	8.544	0.966	0.955	1.123	10.67
Smith	22.640	-7.510	-	-	0.872	0.854	2.020	13.28
Modified Halsey	9.506	-	0.601	-	0.817	0.791	2.420	12.35
Lewicki-2	**13.161**	**0.803**	**-**	**-**	**0.988**	**0.975**	**0.828**	**7.46**
Lewicki-3	10.311	0.302	-24.530	-	0.939	0.919	1.505	11.29
Peleg	**12.440**	**15.650**	**6.179**	**0.284**	**0.995**	**0.986**	**0.628**	**4.22**
Storage temperature 35°C								
Oswin	24.390	0.001	-	-	0.651	0.651	3.076	14.45
Curie	2.200		-	7.346	0.865	0.845	2.048	12.38
Smith	21.991	-7.346	-	-	0.864	0.843	2.048	12.17
Modified Halsey	9.253		0.613	-	0.804	0.776	2.461	13.32
Lewicki-2	**12.68**	**0.799**		**-**	**0.981**	**0.978**	**0.762**	**10.45**
Lewicki-3	11.171	0.237	9.654	-	0.973	0.964	0.976	11.36
Peleg	**12.860**	**14.621**	**5.847**	**0.261**	**0.993**	**0.989**	**0.532**	**6.38**
Storage temperature 40°C								
Oswin	11.740	0.209	-	-	0.971	0.982	0.838	11.65
Curie	1.948	-	-	7.043	0.845	0.821	2.143	12.68
Smith	20.711	-7.043	-	-	0.843	0.826	2.135	14.63
Modified Halsey	7.043	-	-1.948	-	0.844	0.825	2.134	11.29
Lewicki-2	**11.740**	**0.790**	**-**	**-**	**0.981**	**0.978**	**0.738**	**9.57**
Lewicki-3	9.969	0.258	11.480		0.966	0.956	1.061	10.84
Peleg	**13.733**	**12.572**	**5.257**	**0.207**	**0.996**	**0.993**	**0.400**	**5.43**
Storage temperature 45°C								
Oswin	10.971	0.217	-	-	0.974	0.923	0.821	10.10
Curie	1.746	-	-	6.796	0.821	0.795	2.235	11.68
Smith	19.67	-6.796	-	-	0.827	0.7954	2.233	12.62
Modified Halsey	8.393	-	-0.680	-	0.750	0.714	2.639	12.87
Lewicki-2	**10.972**	**0.782**	**-**	**-**	**0.986**	**0.972**	**0.816**	**7.86**
Lewicki-3	9.009	0.277	14.591	-	0.960	0.947	1.138	10.86
Peleg	**10.811**	**14.511**	**4.809**	**0.148**	**0.997**	**0.994**	**0.359**	**3.44**

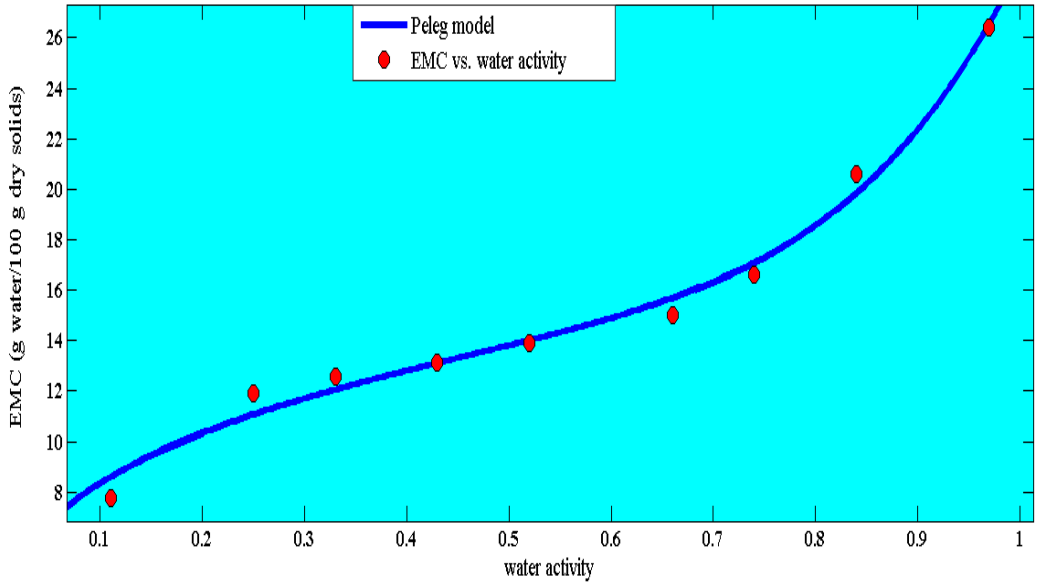

Fig. 6.17a Moisture sorption isotherm predicted by Peleg model at 25^{o}C

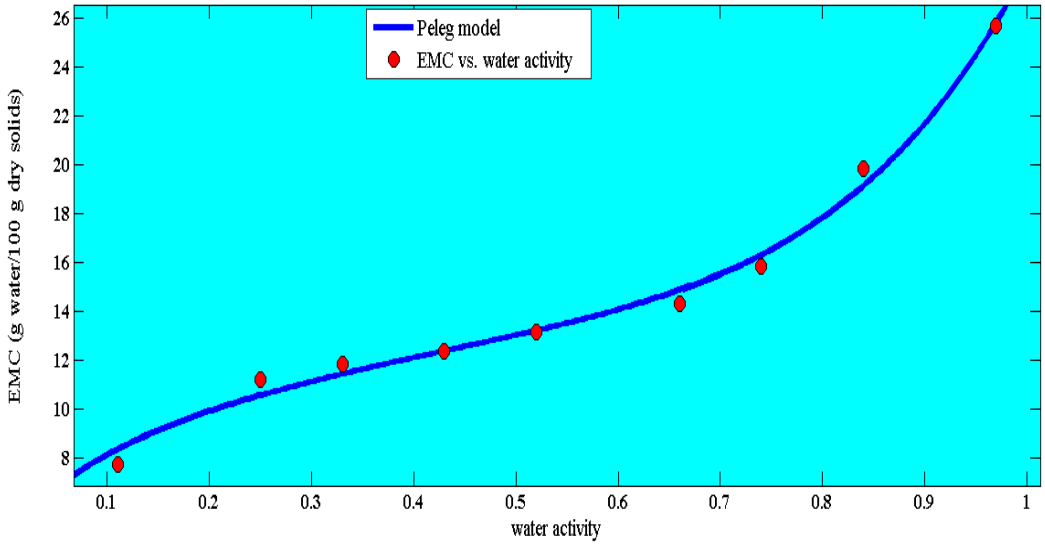

Fig. 6.17b Moisture sorption isotherm predicted by Peleg model at 30^{o}C

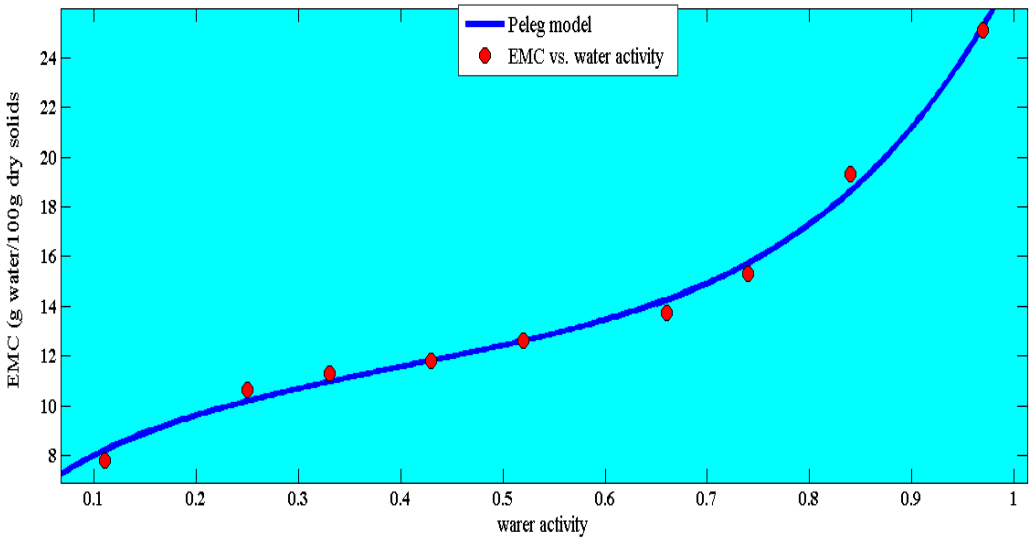

Fig. 6.17c Moisture sorption isotherm predicted by Peleg model at 35^{o}C

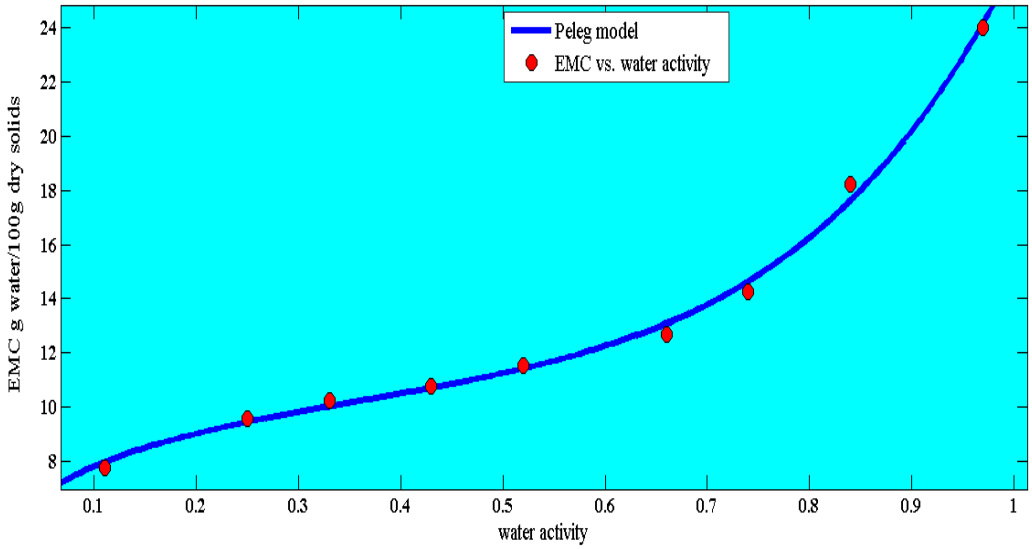

Fig. 6.17d Moisture sorption isotherm predicted by Peleg model at 40^{o}C

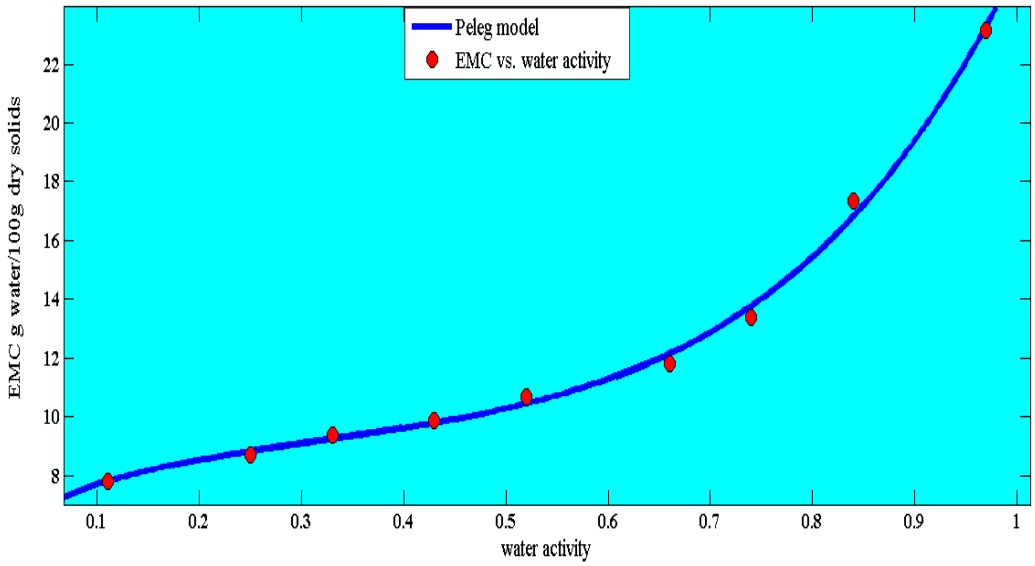

Fig. 6.17e Moisture sorption isotherm predicted by Peleg model at 45^{o}C

6.11.4 Net isosteric heat of sorption

The net isosteric heat of sorption (q_{st}) is used to evaluate the requirements of energy during drying process and provides important information about the state of water in food products.[113] The level of moisture content of material, at which the net isosteric heat of sorption approaches the latent heat of vaporization of water, is often taken as an indication of the amount of 'bound-water' present in the food. As food is dried to lower moisture levels, the heat of vaporization of sorbed water may increase to values above the vaporization of pure water.[114] In the present study, the values of net isosteric heat of sorption as a function of EMC was determined with the help of Eq. (6.28) to the isotherm data by using the best fitted Peleg model. The variation of the net isosteric heat of sorption with respect to EMC is presented in Fig. 6.18. The figure clearly illustrated that the q_{st} values decreased exponentially with an increase in EMC, and decreased to negative at higher moisture content (beyond 60 g water 100 g^{-1} dry solids). The q_{st} value becomes negative due to solubility of sugar sorption phenomenon.[115] In addition, the decrease in q_{st} with the increase EMC values indicates strong water-solid interaction of culinary banana flour in the lower EMC range which decreases with the increase in EMC.[116] At increasing EMC, the most active sites become occupied and sorption occurs on the less active sites giving lower q_{st}.[117] Similar results of decreasing q_{st} with increasing EMC have also been

reported for various foods like potato,[115] coconut press cake[89] and mushroom.[118] Kaymak-Ertekin and Gedik[115] have clearly stated that negative value of q_{st} is purely a mathematical result within the error of determination and has no physical meaning.

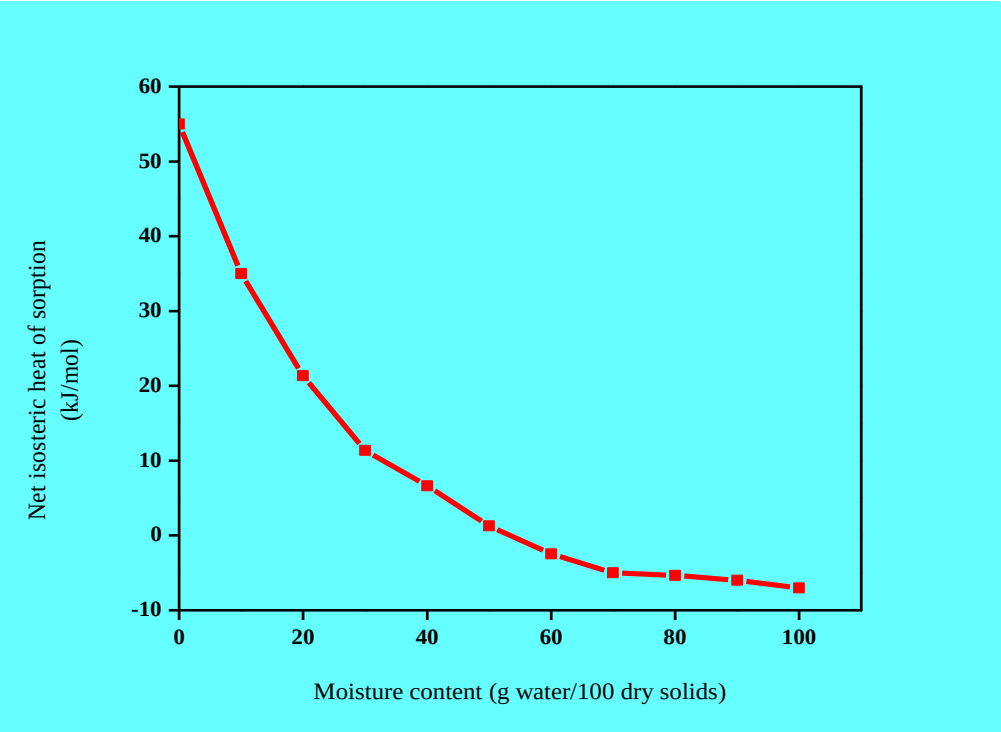

Fig. 6.18 Variation in net isosteric heat of sorption (q_{st}) with equilibrium moisture content (EMC)

6.12 Conclusion

The sorption isotherm study of vacuum dried culinary banana flour conducted at five different temperatures (ranged from 25-45^{o}C) and a_w level (ranged from 0.11-0.97) were evaluated by standard static-gravimetric method using various salt solutions. The obtained isotherm evinced the sigmoid shape resembling type II isotherm which is typical of food material. The experimental sorption data were suitably fitted in four-parameter Peleg model giving highest R^2 and lowest R_d values and indicated good stability at usual storage conditions. On the contrary, in the temperature range studied no significant effect of temperature was noticed on the equilibrium moisture content (EMC) of culinary banana flour. The net isosteric heat of sorption of culinary banana flour revealed decrease in increasing moisture content which

suggested endothermic reaction in the region of lower moisture content. Results favourably support that culinary banana flour can be stored at 25^{o}C up to 120 days with minimal degradation of phenolics and antioxidant activity.

References

1. Mujumdar, S.A., & Law, L C. Drying technology: trends and applications in post harvest processing. *Food Bioprocess Technol.* **3**(6), 843--852, 2010.
2. Tahmasebi, M., et al. Evaluation of thin-layer drying models for simulation of drying kinetics of quercus (*Quercus persica* and *Quercus libani*). *J. Agric. Sci. Technol.* **13** (2), 155--163, 2011.
3. Diamante, L.M., & Yamaguchi, Y. Response surface methodology for optimization of hot air drying of blackcurrant concentrate infused apple cubes. *Int. Food Res. J.* **19**(1), 353--362, 2012.
4. Chakraverty, A., & Singh, R.P. *Post Harvest Technology of Cereals, Pulses And Oilseeds*, Oxford and IBH Publishing Co. Pvt. Ltd., New Delhi, India,1988.
5. Parry, J.L. Mathematical modelling and computer simulation of heat and mass transfer in agricultural grain drying: a review. *J. Agric. Eng. Res.* **32** (1), 1--29, 1985.
6. Ranganna, S. *Handbook of analysis and quality control for fruit and vegetable products*. 2nd ed., Tata McGraw-Hill Publishing Ltd., New Delhi, India, 2008.
7. Tunde-Akintunde, T.Y., & Afon, A.A. Modeling of hot air drying of preheated cassava chips. *Agric. Eng. Int. CIGR J.* **12**(2), 34--41, 2010.
8. Kingsly, R.P., et al. Effects of pretreatments and drying air temperature on drying behaviour of peach slice. *Int. J. Food Sci. Technol.* **42**(1), 65--69, 2007.
9. Lewis, W.K. The rate of drying of solids materials. *Ind. Eng. Chem.* **13**(5), 427--432, 1921.
10. Goyal, R.K., et al. Thin layer drying kinetics of raw mango slices. *Biosyst. Eng.* **95**(1), 43--49, 2006.
11. Doymaz, I. Drying behaviour of green beans. *J. Food Eng.* **69**(2), 161--165, 2005.
12. Page, G.E. *Factors influencing the maximum rate of air drying shelled corn in thin layers*, M.S. Thesis, Department of Mechanical Engineering, Purdue University, Purdue, USA, 1949.
13. Yaldiz, O., et al. Mathematical modeling of thin layer solar drying of sultana grapes. *Energy* **26**(5), 457--465, 2001.
14. Henderson, S.M., & Pabis, S. Grain drying theory I. Temperature effect on drying coefficient. *J. Agric. Eng. Res.* **6**(3), 169--174, 1961.

15. Togrul, I.T., & Pehlivan, D. Mathematical modeling of solar drying of apricot in thin-layers. *J. Food Eng.* **55**(3), 209--216, 2002.
16. Rahman, M.S., et al. Desorption isotherm and heat pump drying kinetics of peas. *Food Res. Int.* **30**(7), 485--491, 1997.
17. Lahsasni, S., et al. Thin layer convective solar drying and mathematical modeling of prickly pear peel (*Opuntia ficus indica*). *Energy* **29**(2), 211--224, 2004.
18. Wang, C.Y., & Singh, R.P. Use of variable equilibrium moisture content in modeling rice drying. *Trans Am. Soc. Agric. Eng.* **11**, 558-572, 1978.
19. Crank, J. *The mathematics of diffusion*, 2nd ed., Oxford University Press, Oxford, 1975.
20. Akpinar, E.K., et al. Single layer drying behaviour of potato slices in a convective cyclone dryer and mathematical modeling. *Energy Convers. Manag.* **44**(10), 1689--1705, 2003.
21. Lopez, A., et al. Thin-layer drying behaviour of vegetable waste from wholesale market. *Drying Technol.* **18**(4-5), 995--1006, 2000.
22. Thuwapanichayanan, R., et al. Determination of effective moisture diffusivity and assessment of quality attributes of banana slices during drying. *LWT--Food Sci. Technol.* **44**(6), 1502--1510, 2011.
23. Alvarez, M., et al. Influence of deformation rate and degree of compression on textural parameters of potato and apple tissues in texture profile analysis. *Eur. Food Res. Technol.* **215**(1), 13--20, 2002.
24. Samaniego-Esguerra, C.M. *Shelf life prediction of dried fruit and vegetables: a quantitative approach.* Ph. D Thesis, Massey University, New Zealand, 1989, 102--105.
25. Brand-Williams, W., et al. Use of a Free Radical Method to Evaluate Antioxidant Activity. *LWT--Food Sci. Technol*. **28**(1), 25--30, 1995.
26. Malick, C.P., & Singh, M.B. *Plant Enzymology and Histo-enzymology*, 4th ed., Kalyani Publishers, New Delhi, 1980.
27. Ertekin, C., & Yaldiz, O. Drying of eggplant and selection of a suitable thin-layer drying model. *J. Food Eng.* **63**(3), 349--359, 2004.
28. Nguyen, H.M., & Price, E.W. Air drying of banana: influence of experimental parameters, slab thickness, banana maturity and harvesting season. *J. Food Eng.* **79**(1), 200--207, 2007.
29. Midilli, A., & Kucuk, H. Mathematical modeling of thin layer drying of pistachio by using solar energy. *Energy Convers. Manage.* **44**(7), 1111--1122, 2003.

30. Abano, E.E., & Sam-Amoah, L.K. Effects of different pretreatments on drying characteristics of banana slices. *ARPN J. Eng. Appl. Sci.* **6**(3), 121--129, 2011.
31. Prachayawarakorn, S., et al. Drying kinetics and quality attributes of low-fat banana slices dried at high temperature. *J. Food Eng.* **85**(4), 509--517, 2008.
32. Srikiatden, J., & Roberts, J.S. Measuring moisture diffusivity of potato and carrot (core and cortex) during convective hot air and isothermal drying. *J. Food Eng.* 74(1): 143--152, 2006.
33. Mitra, J., et al. Vacuum dehydration kinetics of onion slices. *Food Bioprod. Process.* **89**(1), 1--9, 2011.
34. Lertworasirikul S. Drying kinetics of semi-finished cassava crackers: a comparative study. *LWT--Food Sci. Technol.* **41**(8), 1360--1371, 2008.
35. Taheri-Garavand, A., et al. Study on effective moisture diffusivity, activation energy and mathematical modeling of thin-layer drying kinetics of bell pepper. *Aust. J. Crop Sci.* **5**(2), 128--131, 2011.
36. Doymaz, I., & Ismail, O. Drying characteristics of sweet cherry. *Food Bioprod. Process.* **89**(1), 31--83, 2011.
37. Wang, N., & Brennan, J.G. Effect on water binding on drying behaviour of potato, in *Drying*, Mujumdar, A.S. eds., Elsevier Science Publishers, London, 1992, 1350 --1359.
38. Saravacos, G.D., & Charm, S.E. Effect of surface-active agents on the dehydration of fruits and vegetables. *Food Technol.* **16** (1), 91--93, 1962.
39. Zogzas, N.P., et al. Moisture diffusivity data compilation in food stuffs. *Drying Technol.* **14**(10), 2225--2253, 1996.
40. Doymaz, I. Air drying characteristics of tomatoes. *J. Food Eng.* **78**(4), 1291--1297, 2007.
41. Abbasi, S., et al. Investigation of changes in physical and microstructure and mathematical modeling of onion during hot air drying. *Iran Food Sci. Technol. Res. J.* **7**(1), 92--98, 2011.
42. Fazaeli, M., et al. Characterization of food texture: application of Microscopic technology, in *Current Microscopy Contributions to Advances in Science and Technology*, Microscopy Book series Mendez-Vilas, A. eds., US, 2012, 855-871.
43. Karathanos, V.T., & Belessiotis, V.G. Application of a thin-layer equation to drying data of fresh and semi-dried fruits. *J. Agric. Eng. Res.* **74**(4), 355--361, 1999.

44. Brennan, J.G. *Food Dehydration: A Dictionary and Guide*. Oxford Butterworth-Heinemann Ltd., CRC Press, US, 1994.
45. Potter, N.N., & Hotchkiss, J.H. Food Dehydration and Concentration, in *Food Science*, Aspen Publishers Inc., Maryland, 1998; 200--244.
46. Leeratanarak, N., et al. Drying kinetics and quality of potato chips undergoing different drying techniques. *J. Food Eng.* **77**(3), 635--643, 2006.
47. Manuel, S.M., & Sereno, M.A. The kinetics of browning measured during the storage of onion and strawberry. Int. J. Food Sci. Technol. **34**(4), 343--349, 1999.
48. Orikasa, T., et al. Drying characteristics of kiwifruit during hot air drying. *J. Food Eng.* **85**(2), 303--308, 2008.
49. Ozgur, M., et al. Effect of dehydration on several physicochemical properties and the antioxidant activity of leeks (*Allium porrum* L.). *Not. Bot. Horti Agrobot. Cluj-Napoca*, **39**(1), 144--151, 2011.
50. Jangam, S.V. An overview of recent developments and some R&D challenges related to drying of foods. *Drying Technol.* **29**(12), 1343--1357, 2011.
51. Devahastin, S., & Niamnuy, C. Modeling quality changes of fruits and vegetables during drying: A review. *Int. J. Food Sci. Technol.* **45**(9), 1755--1767, 2010.
52. Jeni, K., et al. Design and analysis of the commercialized drier processing using a combined unsymmetrical double-feed microwave and vacuum system (case study: tea leaves). *Chem. Eng. Process.* **49**(4), 389--395, 2010.
53. Das, H. Vacuum Drying, in *Food processing operation analysis,* Asian Books Private Ltd., New Delhi, 2005, 287--304.
54. Jaya, S., & Das, H. A vacuum drying model for mango pulp. *Drying Technol.* **21**(7), 1215--1234, 2003.
55. Omid, M., et al. Modeling drying kinetics of pistachio nuts with multilayer feed forward neural network. *Drying Technol.* **27**(10), 1069--1077, 2009.
56. Banakar, A., & Akandi, K.R.S. Genetic algorithm optimizing approach in rosa petals hot air dryer. *Int. J. Agric. Food Sc.* **2**(3), 60--65, 2012.
57. Hua, C., et al. *Artificial neural network in food processing*. *Proceedings of the 30th Chinese control conference*. Yantai, Chaina, 2011, 2687-2691.
58. Picton, P. *Neural Networks*, 2nd ed., Palgrave, New York, 2000.

59. Watanabe, K., et al. Application of near-infrared spectroscopy for evaluation of drying stress on lumber surface: A comparison of artificial neural networks and partial least squares regression. *Drying Technol.* **32**(5), 590--596, 2014.
60. Murthy, T.P.K., & Manohar, B. Hot air drying characteristics of mango ginger: prediction of drying kinetics by mathematical modeling and artificial neural network. *J. Food Sci. Technol.* **51**(12), 3712--3721, 2013.
61. Erenturk, S., & Erenturk, K. Comparison of genetic algorithm and neural network approaches for the drying process of carrot. *J. Food Eng.* **78**(3), 905--912, 2007.
62. Movagharnejad, K., & Nikzad, M. Modeling of tomato drying using artificial network. *Comput. Electron. Agric.* **59**(1-2), 78--85, 2007.
63. Erenturk, K., et al. A comparative study for the estimation of dynamical drying behaviour of *Echinacea angustifolia*: regression analysis and neural network. *Comput. Electron. Agric.* **45**(1-3), 71--90, 2004.
64. Mohebbi, M., et al. Prediction of moisture content in preosmosed and ultrasounded dried banana using genetic algorithm and neural network. *Food Bioproducts Process.* **89**(4), 362--366, 2011.
65. Morimoto, T. Genetic algorithm, in *Food and Bioprocess Modeling Techniques*, Sablani, S.S., et al. eds., CRC Press, New York, 2006.
66. Aghbashlo, M., et al. Optimization of an artificial neural network topology for predicting drying kinetics of carrot cubes using combined response surface and genetic algorithm. *Drying Technol.* **29**(7), 770--779, 2011.
67. Myers, R.H., & Montgomery, D.C. *Response Surface Methodology: Process and Product Optimization Using Designed Experiments*. John Wiley and Sons, Inc., New York, 2002.
68. Aggarwal, S., et al. A review paper on different encoding schemes used in genetic algorithms. *Int. J. Adv. Res. Comput. Sci. Software Eng.* **4**(1), 596--600, 2014.
69. Prakash, M.J., et al. Box-Behnken design based statistical modeling for ultrasound assisted extraction of corn silk polysaccharide. *Carbohydr. Polym.* **92**(1), 604--611, 2013.
70. Miletic, T., et al. Combined application of experimental design and artificial neural networks in modeling and characterization of spray drying drug: cyclodextrin complexes. *Drying Technol.* **32**(2), 167--179, 2014.

71. Doymaz, I. Drying kinetics and rehydration characteristics of convective hot air dried white button mushroom slices. *J. Chem.* 2014, DOI: http://dx.doi.org/10.1155/2014/453175.
72. Erbay, Z., & Icier, F. Optimization of hot air drying of olive leaves using response surface methodology. *J. Food Eng.* **91**(4), 533--541, 2009.
73. Rigi S., et al. Effect of temperature on drying kinetics, antioxidant capacity and vitamin C content of papaya (*Carica papaya* Linn.). *Int. J. Plant, Anim. Environ. Sci.* **4**(3), 413--417, 2014.
74. Abou-Arab, A.A., et al. Physicochemical properties of natural pigments (anthocyanin) extracted from Roselle calyces (*Hibiscus subdariffa). J. Am. Sci.* **7**(7), 445--456, 2011.
75. Raikham, C., et al. Optimum conditions of fluidized bed puffing for producing crispy banana. *Drying Technol.* **31**(6), 726--739, 2013.
76. Collins, W.W., & Hawtin, G.C. 1999. Conserving and Using Crop Plant Biodiversity in Agroecosystems, in *Biodiversity in Agroecosystems*, Collins, W.W., & Qualset C.O. eds., CRC Press, Boca Raton, Washington, 1999, 267--281.
77. Akubor, P.I., et al. Production and quality evaluation of banana wine. Plant *Foods Hum. Nutr.* **58**(3), 1--6, 2003.
78. Debnath, S., et al. Moisture sorption studies on onion powder. *Food Chem.* **78**(4), 479--482, 2002.
79. Viswanathan, R., et al. Sorption isotherms of tomato slices and onion shreds. *Biosyst. Eng.* **86**(4), 465--472, 2003.
80. Al-Muhtaseb, A.H., et al. Moisture sorption isotherm characteristics of food products: a review. *Food Bioprod. Process.* **80**(2), 118--128, 2002.
81. Cardoso, J. M., & de Silva P.R. Hygroscopic behavior of banana (*Musa* ssp. AAA) flour in different ripening stages. *Food Bioprod. Process.* **92**(1), 73--79, 2014.
82. Peng, G., et al. Modeling of water sorption isotherm for corn starch. *J. Food Eng.* **80**(2), 562--567, 2007.
83. van Der Berg, C., & Bruin, S. Water Activity and Its Estimation in Food Systems: Theoretical Aspects, in *Water Activity: Influences on Food Quality*, Rockland, L.B., & Stewart, G.F. eds., Academic Press, London, UK, 1981, 189--200.

84. Bezerra, C.V., et al. Green banana (*Musa cavendishii*) flour obtained in spouted bed - effect of drying on physico-chemical, functional and morphological characteristics of the starch. *Ind. Crops Prod.* **41**, 241--249, 2013.
85. Chiste, R.C., et al. Sorption isotherms of tapioca flour. *Int. J. Food Sci. Technol.* **47**(4), 870--874, 2012.
86. Cova, A., et al. The effect of hydrophobic modifications on the adsorption isotherms of cassava starch. *Carbohydr. Polym.* **81**(3), 660--667, 2010.
87. Mishra, S., & Rai, T. Morphology and functional properties of corn, potato and tapioca starches. *Food Hydrocolloids* **20**(5), 557--566, 2006.
88. Sant'anna, V., et al. Grape marc powder: Physicochemical and microbiological stability during storage and moisture sorption isotherm. *Food Bioprocess Technol*. **7**(9), 2500--2506, 2014.
89. Jena, S., & Das, H. Moisture sorption studies on vacuum dried coconut presscake. *J. Food Sci. Technol.* **49**(5), 638--642, 2012.
90. Jha, E., et al. Moisture sorption characteristics of gluten-free flour. *Int. J. Agric. Food Sci. Technol.* **5**(2), 27--34, 2014.
91. Oyerinde, A.S. Determination of moisture sorption isotherm characteristics of dehydrated sorghum flour ("Ogi"). *J. Agric. Sci. Technol.* **B3**, 86--91, 2013.
92. Yan, Z., et al. Sorption isotherms and moisture sorption hysteresis of intermediate moisture content banana. *J. Food Eng.* **86**(3), 342--348, 2008.
93. Cassini, A.S., et al. Water adsorption isotherms of texturized soy protein. *J. Food Eng.* **77**(1), 194--199, 2006.
94. Sahin, S., & Sumnu, S.G. Water Activity and Sorption Properties of Foods, in *Physical Properties of Foods*, Sahin, S., & Sumnu, S.G. eds., Springer Science+Business Media, New York, 2006,193-226.
95. Greenspan, L. Humidity fixed points of binary saturated aqueous solutions. J. Res. Natl. Bur. Stand., Sect. A **81**(1), 89--96, 1977.
96. Andrade, P.R.D., et al. Models of sorption isotherms for food: Uses and limitations. *Vitae Rev. De La Fac. De Quomica Farm.* **18**(3), 325-- 334, 2011.

97. Caurie, M. Derivation of full range moisture isotherms, in *Water Activity: Influences on Food Quality*, Rockland, L.B., & Stewart, G.F. eds., Academic Press, New York, 1981, 63--87.
98. Basu, S., et al. Models for sorption isotherms for foods: a review. *Drying Technol.* **24**(8), 917--930, 2006.
99. Lewicki, P.P. The applicability of the GAB model to food water sorption isotherms. *Int. J. Food Sci. Technol.* **32**(6), 553--557, 1997.
100. Lewicki, P.P. A three parameter equation for food moisture sorption isotherms. *J. Food Process Eng.* **21**(2), 127--144, 1998.
101. Sircar, S., et al. Isosteric Heat of Adsorption: theory and Experiment. *J. Phys. Chem. B*, **103**(31), 6539--6546, 1999.
102. Yousif, A.N., et al. Headspace volatiles and physical characteristics of vacuum microwave, air, and freeze-dried oregano (*Lippiaber landieri* Schauer). *J. Food Sci.* **65**(6), 926--930, 2000.
103. Mundada, M., & Hathan, B.S. Studies on moisture sorption isotherms for osmotically pretreated and air-dried pomegranate arils. *J. Food Process. Preserv.* **36**(4), 329--338, 2012.
104. Doporto, M.C., et al. Physicochemical, thermal and sorption properties of nutritionally differentiated flour and starches. *J. Food Eng.* **113**(4), 569--576, 2012.
105. Fan, K., et al. Moisture adsorption isotherms and thermodynamic properties of *Auricularia auricular*. *J. Food Process. Preserv.* DOI:10.1111/jfpp.12379.
106. Wang, X., et al. Moisture adsorption isotherms and heat of sorption of *Agaricus bisporus*. *J. Food Process. Preserv.* **37**(4) 299--305, 2013.
107. Cladera-Olivera, F., et al. Modeling water adsorption isotherms of *pinhao* (*Araucaria angustifolia* seeds) flour and thermodynamic analysis of the adsorption process. *J. Food Process Eng.* **34**(3), 826--843, 2011.
108. Perdomo, J., et al. Glass transition temperatures and water sorption isotherms of cassava starch. *Carbohydr. Polym.* **76**(2), 305--313, 2009.
109. Johnson, P.-N.T., & Brennan, J.G. Moisture sorption isotherm characteristics of plantain (*Musa* AAB). *J. Food Eng.* **44**(2), 79--84, 2000.
110. Montes, E., et al. Models of desorption isotherms of yam (*Dioscorearotundata*). *Dyna* **72**(157), 145--152, 2009.

111. Iguedjtal, T., et al. Sorption isotherms of potato slices dried and texturized by controlled sudden decompression. *J. Food Eng.* **85**(2), 180--190, 2008.
112. Hayoglu, I., & Faruk, O.G. Water sorption isotherms of pistachio nut paste. *Int. J. Food Sci. Technol.* **42**(2), 224--227, 2007.
113. Aktas, T., et al. Sorption isotherms and net isosteric heat of sorption for plum osmotically pre-treated with trehalose and sucrose solutions. *Bulg. J Agric. Sci.* **20**(3), 515--522, 2014.
114. Yazdani, M., et al. Moisture sorption isotherms and isosteric heat for pistachio. Eur. Food Res. Technol. **223**(5), 577--584, 2006.
115. Kaymak-Ertekin, F., & Gedik, A. Sorption isotherms and isosteric heat of sorption for grapes, apricots, apples and potatoes. *LWT--Food Sci. Technol.* **37**(4), 429--438, 2004.
116. Nourhene, B., et al. Sorption isotherms and isosteric heats of sorption of olive leaves (*Chemlali* variety): Experimental and mathematical investigations. *Food Bioprod. Process.* **86**(3), 167--175, 2008.
117. Quirijns, E.J., et al. Sorption isotherms, GAB parameters and isosteric heat of sorption. *J. Sci. Food Agric.* **85**(11), 1805--1814, 2005.
118. Hossain, M.D., et al. Sorption isotherms and heat of sorption of pineapple. *J. Food Eng.* **48**(2), 103--107, 2001.